

NASA CR-139172

WIDEBAND INFRARED HETERODYNE RECEIVER FRONT-END

B. J. Peyton

August 1974
FINAL REPORT

(NASA-CR-139172) WIDEBAND INFRARED
HETERODYNE RECEIVER FRONT-END Final Report
(Airborne Instruments Lab.) 55 p 8

N75-14937

CSCC 11/B

Unclas

G3/32 06964

Prepared for:
Goddard Space Flight Center
Greenbelt, Maryland 20771



Reproduced by
NATIONAL TECHNICAL
INFORMATION SERVICE
US Department of Commerce
Springfield, VA. 22151

AIL a division of
CUTLER-HAMMER
MELVILLE, LONG ISLAND, NEW YORK 11746



PRICES SUBJECT TO CHANGE

1. Report No.	2. Government Accession No.	3. Recipient's Catalog No.	
4. Title and Subtitle WIDEBAND INFRARED HETERODYNE RECEIVER FRONT END		5. Report Date August 1974	
		6. Performing Organization Code	
7. Author(s) B. J. Peyton and J. Wolczok		8. Performing Organization Report No. 7886-1	
9. Performing Organization Name and Address AIL, a division of Cutler-Hammer Melville, New York 11746		10. Work Unit No.	
		11. Contract or Grant No. NAS-5-23119	
12. Sponsoring Agency Name and Address Goddard Space Flight Center Greenbelt, Maryland 20771		13. Type of Report and Period Covered Final Report	
		14. Sponsoring Agency Code	
15. Supplementary Notes			
16. Abstract <p>A 10.6 μm infrared heterodyne receiver front end has been developed for use in a wideband CO₂ laser communications link. The infrared receiver employs an 850 MHz response PV HgCdTe photo-mixer which is mounted in a space quality housing, a low-noise 5 to 1500 MHz IF preamplifier, and a remote control panel. The receiver has been designed to handle ± 750 MHz of Doppler shift while providing an instantaneous information bandwidth of 400 MHz. The measured receiver sensitivity NEP was 1.0×10^{-19} W/Hz for a photomixer temperature of $T_m = 77$ K and an IF beat frequency of 20 MHz and degraded to 1.75×10^{-19} W/Hz for $T_m = 130$ K.</p>			
17. Key Words Wideband Heterodyne Receivers Optical Communications CO ₂ Laser Receiver		18. Distribution Statement	
19. Security Classif. (of this report) UNCLASSIFIED	20. Security Classif. (of this page) UNCLASSIFIED	21. No. of Pages 52	22. Price

ACKNOWLEDGMENTS

AIL staff members R. Lange and M. Savage made contributions to the reported measurements. This work was carried out in the Infrared and Electro-Optics Department under F. P. Pace, Department Head.

TABLE OF CONTENTS

	<u>Page</u>
I. Introduction	1
II. Optimization of Infrared Heterodyne Receiver Components	5
A. Photomixer Characteristics	5
B. Photomixer Contact (1/F) Noise	7
C. Laser LO Induced Shot Noise	8
D. Photomixer Cutoff Frequency	10
E. Photomixer Housing	16
F. IF Preamplifier	16
III. Heterodyne Receiver Performance	19
A. Receiver Sensitivity	19
B. Laser Local Oscillator Power	24
C. Dc Bias Power	26
IV. Heterodyne Receiver Performance at Elevated Photomixer Temperature	27
A. Photomixer Characteristics	27
B. Laser LO Induced Photocurrent	30
C. Photomixer Cutoff Frequency	30
D. Receiver Sensitivity	33
V. Packaged Receiver	39
A. Variable Temperature Cooler	39
B. Photomixer-IF Preamplifier Control Panel	40
C. Operating Levels	40
VI. Conclusions	45
VII. References	49

PRECEDING PAGE BLANK NOT FILMED

LIST OF ILLUSTRATIONS

<u>Figure</u>		<u>Page</u>
1	Simplified Representation of IF Requirements for an Infrared Heterodyne Receiver in a Satellite-to-Satellite CO ₂ Laser Communications Link	3
2	Current Versus Voltage (I-V) Characteristic of a Wideband PV HgCdTe Photomixer	6
3	Measured Reverse Shunt Resistance of Wideband PV HgCdTe Photomixer for the Case of No Applied Laser LO Power	6
4	Current-Voltage (I-V) Characteristic of Wideband PV HgCdTe Photomixer With and Without Applied Laser LO Power	7
5	Photomixer Noise Versus Frequency of Wideband PV HgCdTe Photomixer	9
6	Measured Frequency Response of Photomixer/Preamplifier Combination with Bias Voltage as a Parameter	11
7	Measured 3-dB Cutoff Frequency Versus Bias Voltage for Wideband PV HgCdTe Photomixer	13
8	Measured Frequency Response of a Photomixer Housing	14
9	Space Quality Photomixer Housing	17
10	Measured Heterodyne Receiver Sensitivity for $V_B = -400$ and -800 mV	21
11	Measured Heterodyne Receiver Sensitivity of PV HgCdTe Photomixer/IF Preamplifier as a Function of Photoinduced Current	25
12	Measured Current Voltage Characteristics of a Wideband PV HgCdTe Photomixer at 77 K and 130 K	28
13	Photomixer Slope Resistance Versus Temperature with Reverse Bias Voltage as a Parameter	29

<u>Figure</u>		<u>Page</u>
14	Maximum Laser LO Induced Photocurrent as a Function of Photomixer Temperature with Photomixer Bias Voltage as a Parameter	31
15	Measured 3-dB Cutoff Frequency Versus Bias Voltage for Wideband PV HgCdTe Photomixer	32
16	Heterodyne Receiver NEP Versus IF with Photomixer Temperature as a Parameter	34
17	Measured Heterodyne Receiver Sensitivity as a Function of Applied Photomixer Bias Voltage with Photomixer Temperature as a Parameter	35
18	Measured Reverse Current Characteristic of a Wide-band PV HgCdTe Photomixer at 97 K and 140 K	36
19	Photomixer Cooler with IF Preamplifier and IF Post-amplifier	42
20	Photomixer Housing Mounted in Variable Temperature Cooler	43
21	Remote Control Panel and Power Supplied	44
22	Complete CO ₂ Laser Communications Receiver	46
23	Complete CO ₂ Laser Communications Receiver Mounted in Laboratory Test Setup	47

LIST OF TABLES

<u>Table</u>	<u>Page</u>
I Variation of PV HgCdTe Photomixer Characteristics with Applied Bias Voltage	12
II Calculated Affect of Shunt Conductance Variations on Photomixer 3-dB Frequency Response	15
III Measured Infrared Heterodyne Receiver Sensitivity for a PV HgCdTe Photomixer Temperature of 77 K and a 20-MHz IF Offset	23
IV Variation of PV HgCdTe Photomixer 3-dB Cutoff Frequency as a Function of Bias Voltage and Mixer Temperature	33
V Measured Heterodyne Receiver Sensitivity at Photomixer Temperatures between 77 K and 137 K for IF = 20 MHz and $V_B = -400$ mV	34
VI Measured Heterodyne Receiver Sensitivity at Photomixer Temperatures Between 77 and 147 K for IF = 20 MHz and $V_B = -800$ mV	37

PREFACE

This is the final report on Contract NAS-5-23119, entitled "Wideband Infrared Heterodyne Receiver Front-End." The program is aimed at the development, fabrication, and test of a 10.6- μ m infrared heterodyne receiver for use in a CO₂ laser communications link. The infrared receiver employs a wideband PV HgCdTe photomixer which is mounted in a space quality housing and exhibits a 3-dB cutoff frequency of 850 MHz for an applied bias voltage of $V_B = -800$ mV. A low-noise IF preamplifier amplifies the beat frequency output of the photomixer, provides 40 dB of gain and operates between 5 and 1500 MHz. The receiver has been designed to handle ± 750 MHz of Doppler frequency shift while providing an instantaneous information bandwidth of 400 MHz.

Photomixer and receiver characteristics have been tested over the 5 to 1500 MHz IF band and a photomixer temperature range between $T_m = 77$ and 140 K to permit selection of an optimum set of operating conditions. The measured receiver sensitivity for IF = 20 MHz and $V_B = -800$ mV is 1×10^{-19} W/Hz at $T_m = 77$ K and increases to 1.75×10^{-19} W/Hz at $T_m = 130$ K. For IF = 1500 MHz and $V_B = -800$ mV, the receiver NEP is 1.65×10^{-19} W/Hz at $T_m = 77$ K and increases to 3×10^{-19} W/Hz at $T_m = 130$ K.

I. INTRODUCTION

This is the final report on Contract NAS-5-23119 entitled "Wideband Infrared Heterodyne Receiver Front-End." The program is aimed at the development, fabrication, and test of a 10.6- μ m infrared heterodyne receiver which provides nearly quantum-noise-limited sensitivity, exhibits an IF response up to 1500 MHz, and operates at photomixer temperatures between 77 K and 130 K.

This wideband heterodyne receiver has been designed for use in an engineering model of a simulated CO₂ laser spaceborne communications link. For the link considered, the CO₂ laser transmitter and the CO₂ laser local oscillator (LO) are operated on the same laser transition. For low-altitude-satellite to synchronous-satellite and low-altitude-satellite to ground links, the transmitted laser signal is Doppler-shifted due to the relative velocity of the low-altitude satellite with respect to the ground station or with respect to the synchronous-orbit satellite (reference 1). The resultant Doppler frequency shift varies with time and, hence, must be frequency tracked by either (a) a spectrally wide laser LO which can be rapidly tuned at infrared wavelengths, or (b) a heterodyne receiver which employs a fixed frequency laser LO and a wideband IF network which can be rapidly scanned using RF techniques. This latter type of communications receiver which utilizes IF tuning to handle the Doppler frequency offset is adopted here as described in this report. The design of wideband infrared heterodyne receivers has been previously considered under NASA sponsorship (reference 2). An electronic receiver back-end, also developed at AIL under NASA contract* accepts the output of the heterodyne receiver front end and tracks the Doppler shifted signal so as to maintain a constant second IF at 1500 MHz. The receiver has a 400 MHz instantaneous IF bandwidth with a 300 mega bit data capacity, and provides the required demodulation circuitry. An RF Doppler simulator which provides a calibrated RF signal with appropriate Doppler shifts and bit error rates has been developed** and used to evaluate the performance of the infrared heterodyne receiver back end.

* The Doppler tracking receiver back-end was developed under Contract NAS-5-23183 (reference 3).

** The RF Doppler Simulator was developed under Contract NAS-5-23211.

Figure 1 is a simplified representation of a low-altitude satellite-to-ground optical communications link. A maximum positive Doppler offset is experienced as the satellite is acquired as it comes up over the horizon. The offset then goes through a minimum while the satellite is over the ground station (the zenith position) and thereafter increases negatively as the satellite recedes from the ground station. Maximum Doppler offsets of $\Delta f_d = \pm 750$ MHz and IF information bandwidths of ± 200 MHz have been considered for this application.

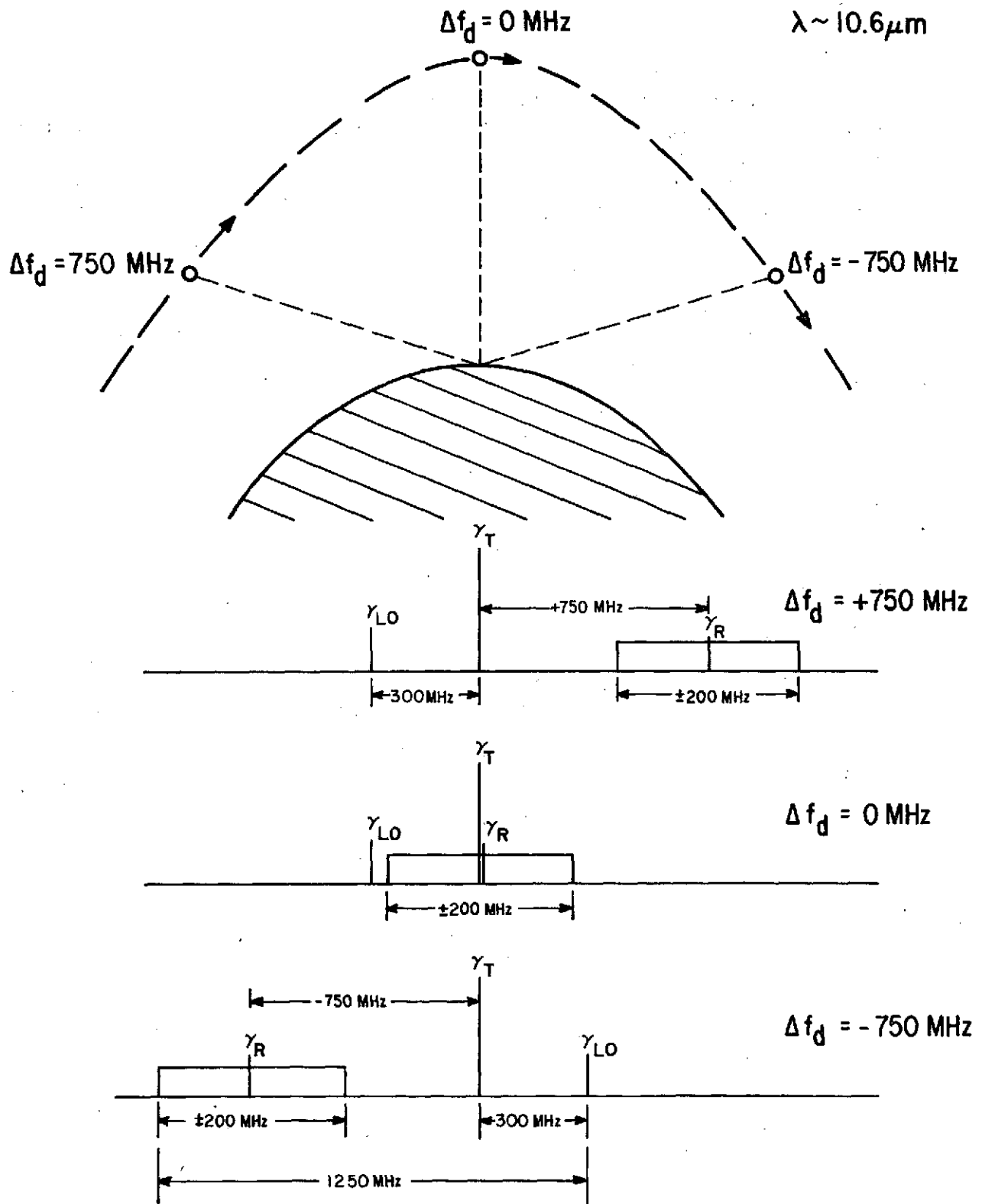
In order to prevent communication data distortion due to data foldover when $\Delta f_d < 200$ MHz, the laser LO in the heterodyne receiver front end is frequency offset by a minimum of 200 MHz with respect to the frequency of the laser transmitter (Figure 1). As the satellite passes through the zenith position, the polarity of the laser LO offset frequency is reversed with respect to the laser transmitter frequency.

Measured data on the electronic back end of the infrared heterodyne communications receiver (reference 3) indicates that the system bit error rate for an IF offset of 300 MHz between the Doppler shifted transmitter carrier frequency and the receiver laser LO frequency is approximately two orders of magnitude lower than can be obtained from an IF offset of 200 MHz. Therefore, for a communications link having a maximum Doppler frequency of 750 MHz, an IF bandwidth of ± 200 MHz to handle a 300 mega-bit data stream, as well as an IF offset of 300 MHz between the received carrier frequency and the LO frequency, a heterodyne receiver with an IF response up to 1250 MHz is required (Figure 1).

Based on these considerations, the program objectives for this wide-band infrared heterodyne receiver front-end development were set as follows:

Optical Wavelength	10.6 μ m (P-20 line of CO ₂ laser)
IF Response	10 to 1500 MHz
Photomixer Operating Temperature	77 to 130 K
Receiver Sensitivity	$\leq 2 \times 10^{-19}$ W/Hz, IF ≤ 300 MHz $\leq 5 \times 10^{-19}$ W/Hz, IF ≤ 1500 MHz

The wideband infrared heterodyne receiver front-end developed on this program meets all the objective specifications. The wideband PV HgCdTe photomixer has been mounted in a space quality housing which is fastened to a variable temperature cooler. In addition, a wideband preamplifier has been matched to the photomixer and a remote control panel has been developed.



V73-2674R1

Figure 1. Simplified Representation of IF Requirements for an Infrared Heterodyne Receiver in a Satellite-To-Satellite CO₂ Laser Communications Link

Heterodyne receiver measurements have been carried out over the 77 to 130 K temperature range to simulate operation in a passive radiative cooler which might be employed in an operational satellite receiver system. Measured results indicate that efficient heterodyne operation can be obtained at photomixer temperatures up to 130 K.

II. OPTIMIZATION OF INFRARED HETERODYNE RECEIVER COMPONENTS

Key parameters which affect wideband operation in a 10.6 μm heterodyne receiver using PV HgCdTe photomixers cooled to 130 K have been theoretically investigated. In addition, photomixer characteristics as a function of operating temperature T_M , applied bias voltage V_B , and incident laser LO power P_{LO} have been measured. As a result, an optimum set of operating conditions for wideband heterodyne receiver operation have been determined. A wideband low-noise IF preamplifier matching the impedance characteristics of the photomixer has been fabricated, and provides 40 dB of IF gain over the 10 to 1500 MHz IF range.

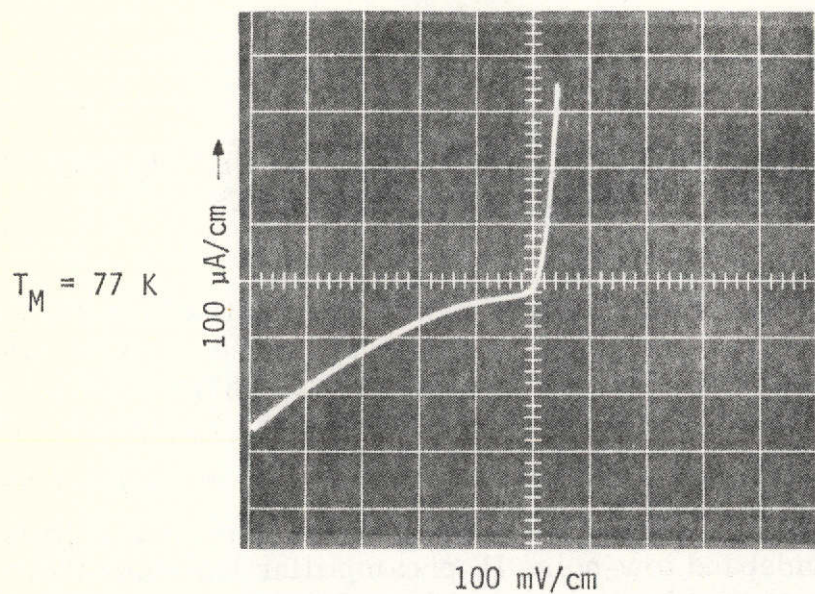
A. PHOTOMIXER CHARACTERISTICS

A high speed PV:HgCdTe photomixer mounted in an AIL/SAT developed space quality housing (reference 4) is employed as the detection element in the 10.6- μm heterodyne receiver package. The PV:HgCdTe photomixer has the following characteristics at $T_M = 77$ K:

Sensitive Area	$\sim 4 \times 10^{-4} \text{ cm}^2$
Peak Spectral Response	$\sim 10.85 \mu\text{m}$
Series Resistance, R_S	$\sim 34 \text{ ohms}$
Detectivity, D^*	$2.5 \times 10^{10} \text{ cm Hz}^{1/2} \text{ W}^{-1}$
Maximum Photocurrent	1.5 ma

Figure 2 shows the measured current versus voltage (I-V) characteristics at $T_M = 77$ K. As may be seen, the reverse shunt resistance G_D^{-1} of the photomixer varies from approximately 4 kilohms at an applied bias voltage of $V_B = -100$ mV to 900 ohms at $V_B = -800$ mV. Figure 3 shows the measured variation of photomixer shunt resistance with reverse bias voltage.

Figure 4 shows the photomixer I-V characteristic with and without applied CO_2 laser power for the condition of a laser LO induced photocurrent



4-2572

Figure 2. Current Versus Voltage (I-V) Characteristic of a Wideband PV HgCdTe Photomixer

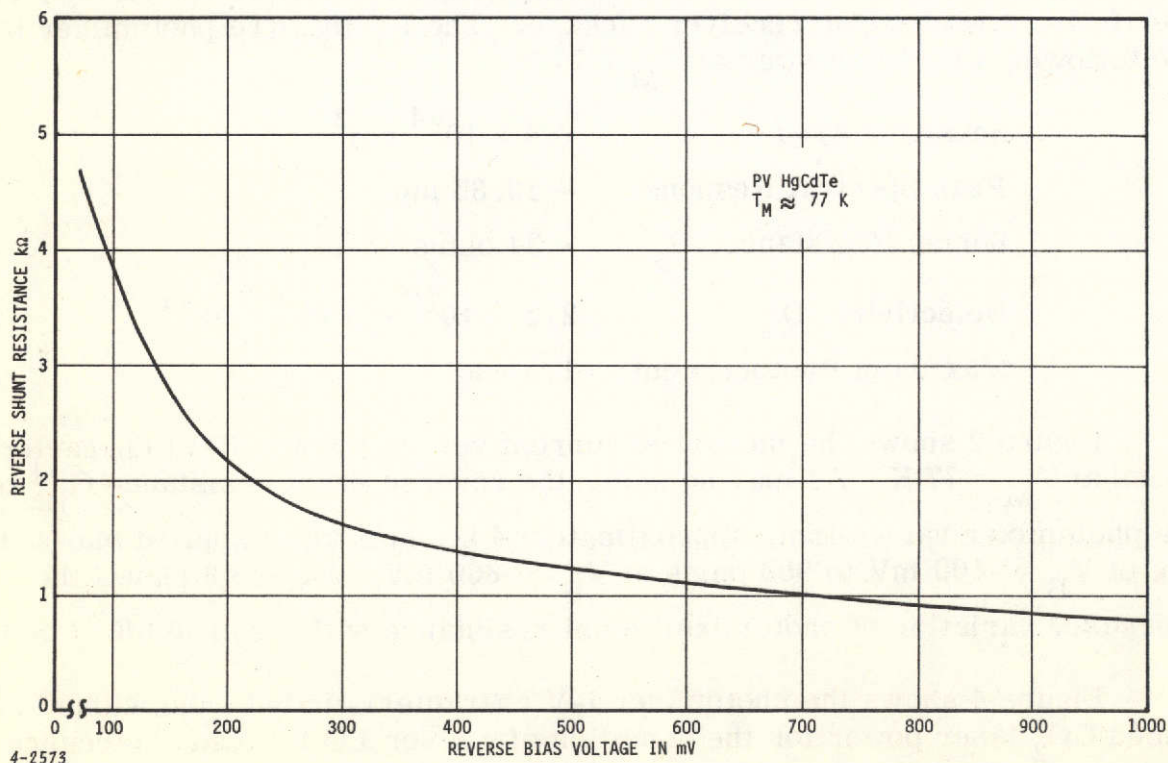
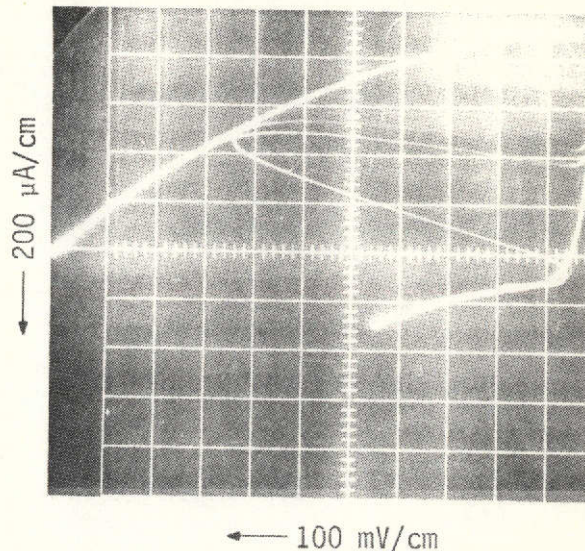


Figure 3. Measured Reverse Shunt Resistance of Wideband PV HgCdTe Photomixer for the Case of No Applied Laser LO Power

$T_M = 77 \text{ K}$
 $I_0 \approx 1.1 \text{ mA}$
 $\lambda = 10.59 \text{ } \mu\text{m (P-20)}$



4-2574

Figure 4. Current-Voltage (I-V) Characteristic of Wideband PV HgCdTe Photomixer With and Without Applied Laser LO Power

of $I_0 = 1.1 \text{ mA}$. Measured data indicates that the photomixer shunt conductance changes only slightly with variations in the applied laser LO power. It is, however, a significant parameter in the design considerations of the low noise IF preamplifier.

B. PHOTOMIXER CONTACT (1/F) NOISE

In order to evaluate the excess noise in the detector, measurements were carried out on the PV HgCdTe photomixer at a temperature of 77 K in the absence of a local oscillator at IF's between 100 kHz and 20 MHz and applied bias voltages between 0 and 1 volt. The measured contact (1/f) photomixer noise (Figure 5) is relatively unaffected by applied laser LO power, but is expected to increase with increasing dc bias voltage and decreasing frequency according to the relationship

$$V_N^2 = \frac{K V_B^2 B}{f^\alpha V} \quad (1)$$

where:

K = proportionality constant

V_B = dc bias voltage

B = bandwidth

f = frequency

$\alpha = 1$ in the lower frequency region

V = photomixer volume

Measured data indicates that for IF's above 1 MHz, the contact (1/f) noise is approximately equal to the IF amplifier noise for bias voltages up to $V_B = -1$ volt.

C. LASER LO INDUCED SHOT NOISE

In a heterodyne receiver, absorbed photons from the laser LO generate hole-electron pairs which are collected at the terminals of the photodiode. The induced photocurrent (Figure 4) is given by

$$I_O = \frac{\eta q P_{LO}}{h\nu} \quad (2)$$

where:

η = photomixer quantum efficiency

q = electronic charge

P_{LO} = incident laser LO power

h = Planck's constant

ν = infrared frequency

The LO induced photocurrent gives rise to a mean-square shot noise current given by

$$\bar{i}_s^2 = 2 q I_O B, \quad \text{for} \quad f_{if} < 1/8 T_r \quad (3)$$

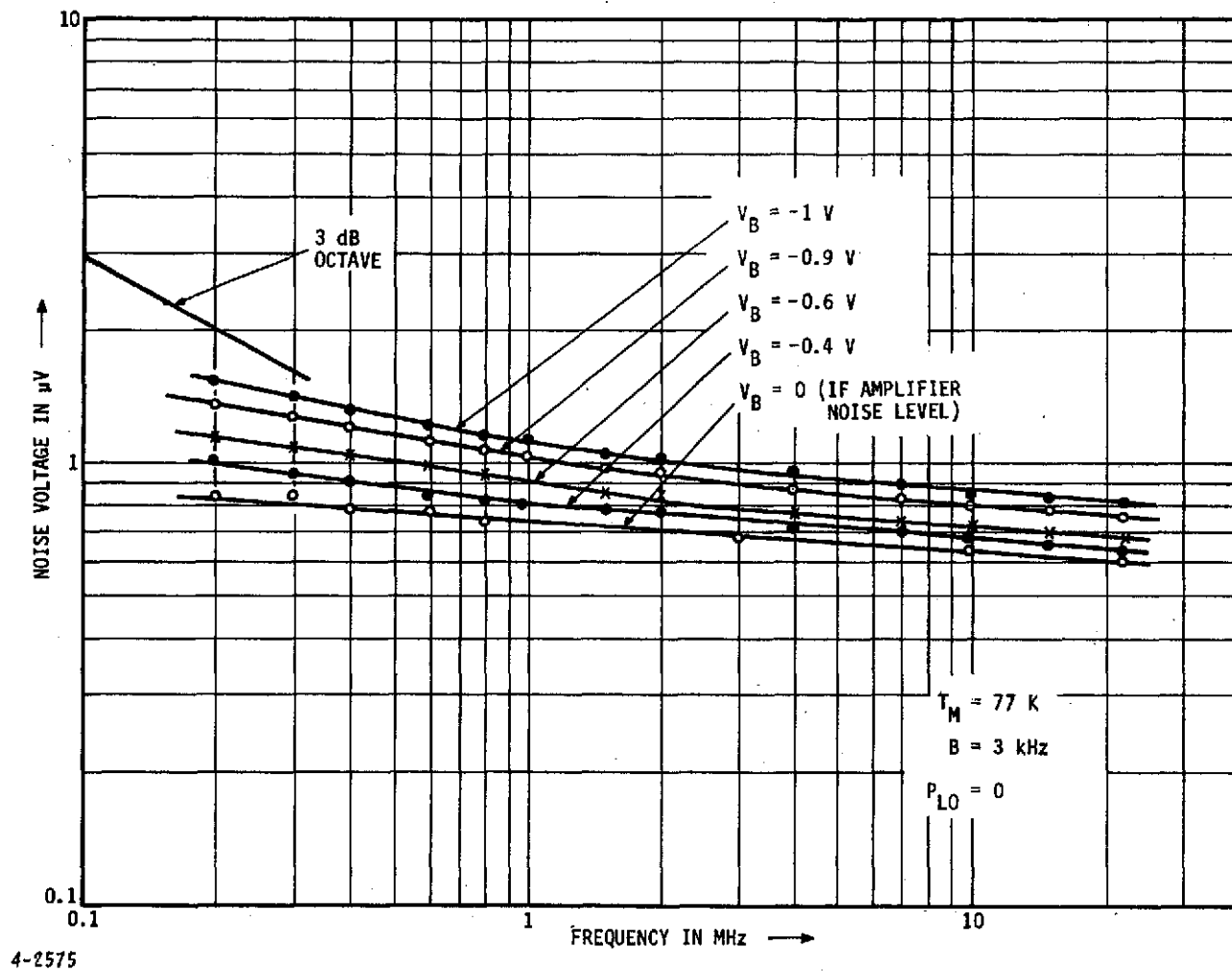


Figure 5. Photomixer Noise Versus Frequency of Wideband PV HgCdTe Photomixer

where B is the IF bandwidth and T_r is the photomixer transit time. For a fixed applied laser LO power, the shot noise power spectrum at the output of the heterodyne receiver is expected to be constant with the IF. By measuring the noise power at the output of the heterodyne receiver, the apparent rolloff in the system shot noise can be used to determine the frequency response of the photomixer (references 2 and 5). This technique was used in measuring the frequency response of the receiver.

D. PHOTOMIXER CUTOFF FREQUENCY

The 3-dB cutoff frequency of an RC limited reverse biased photovoltaic photomixer is given (reference 2) by

$$f_c = \frac{(1 + R_S G_D)^{1/2}}{2\pi C_D (R_S/G_D)^{1/2}} \quad (4)$$

$$\approx \frac{G_D^{1/2}}{2\pi C_D R_S^{1/2}}, \quad R_S G_D \ll 1 \quad (5)$$

where

R_S = photomixer series resistance

G_D = small-signal shunt conductance of the photomixer

C_D = photomixer junction capacitance

Frequency response measurements have been carried out on the wide-band HgCdTe photomixer and a matched IF preamplifier at applied dc bias voltages (V_B) between -200 and -1000 mV. Figure 6 gives the measured photomixer response for $V_B = -300$ and -600 mV and the complete data is summarized in Table I. As shown, the measured 3-dB cutoff frequency was 310 MHz at $V_B = -200$ mV and increased to 970 MHz at $V_B = -1$ volt.

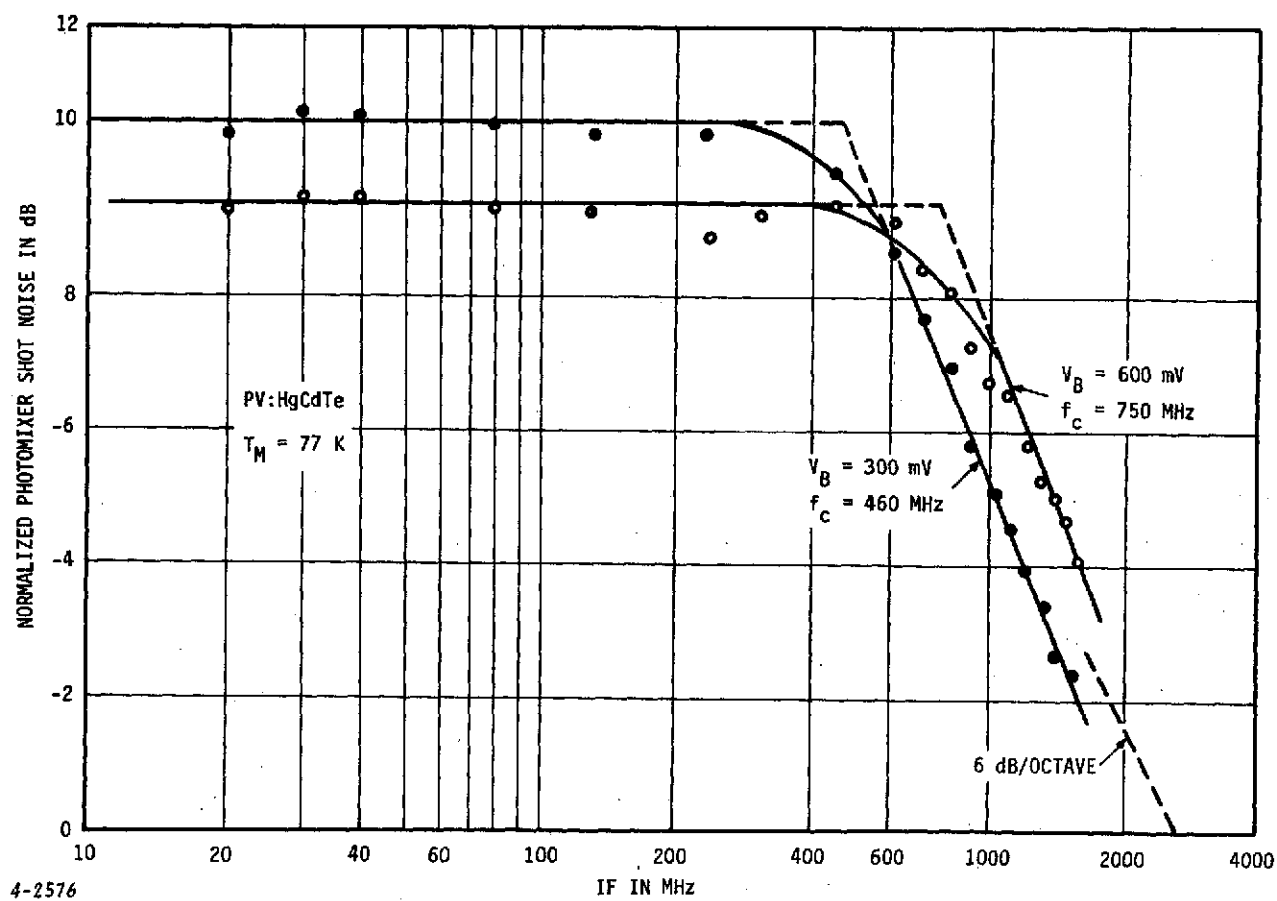


Figure 6. Measured Frequency Response of Photomixer/Preamplifier Combination with Bias Voltage as a Parameter

TABLE I. VARIATION OF PV HgCdTe PHOTOMIXER CHARACTERISTICS
WITH APPLIED BIAS VOLTAGE

<u>Applied Voltage*</u>	<u>Reverse Conductance</u>	<u>Cutoff Frequency</u>
V_B (mV)	G_D^{-1} (ohms)	f_c (MHz)
-200	2100	~310
-300	1600	~460
-400	1400	~560
-600	1125	~750
-800	900	~850
-1000	750	~970

* The maximum applied bias voltage for this photomixer is -1500 mV.

Figure 7 shows the variation of photomixer cutoff frequency with reverse bias. For bias voltages between -200 and -400 mV, the photomixer cutoff frequency appears to vary as $(V_B)^N$ where N = a constant. While above $V_B = -400$ mV, the photomixer response varies more slowly with applied bias voltage. This apparent observed "saturation" effect may be caused by either of the following:

- The effect of the natural cutoff frequency of the photomixer housing. A similar photomixer housing was evaluated under NASA sponsorship (reference 4) and found to have a natural cutoff frequency near 1200 MHz (Figure 8)
- The effect of the change in reverse photomixer shunt conductance with applied bias voltage (equation 4 and Table I). Table II summarizes the calculated effect of the changing shunt conductance on the photomixer 3-dB cutoff frequency and the measured deviation from the expected $f_c = K (V_B)^N$ relationship which occurs when the photomixer cutoff frequency is limited by the RC constant of the diode junction. The calculated and measured deviation from the normalized cutoff frequency at $V_B = -400$ mV were in fairly good agreement over the -300 to -1000 mV bias interval.

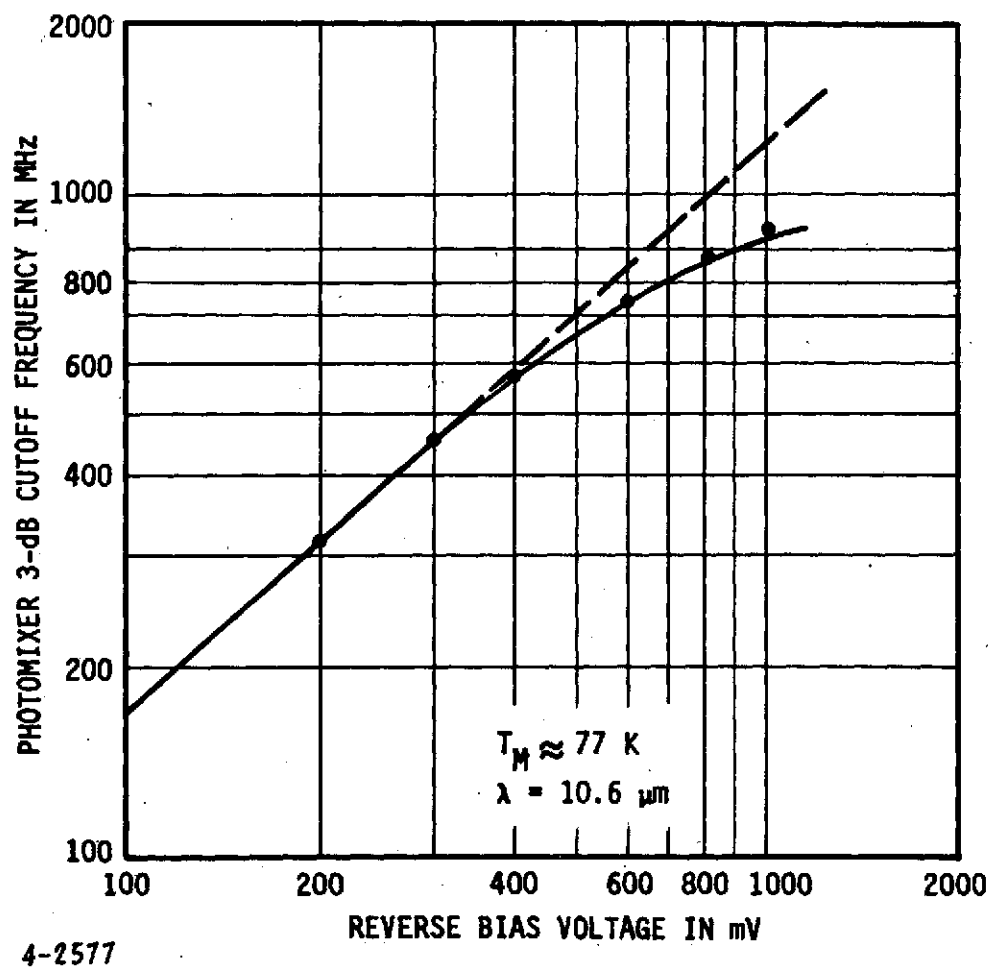


Figure 7. Measured 3-dB Cutoff Frequency Versus Bias Voltage for Wideband PV HgCdTe Photomixer

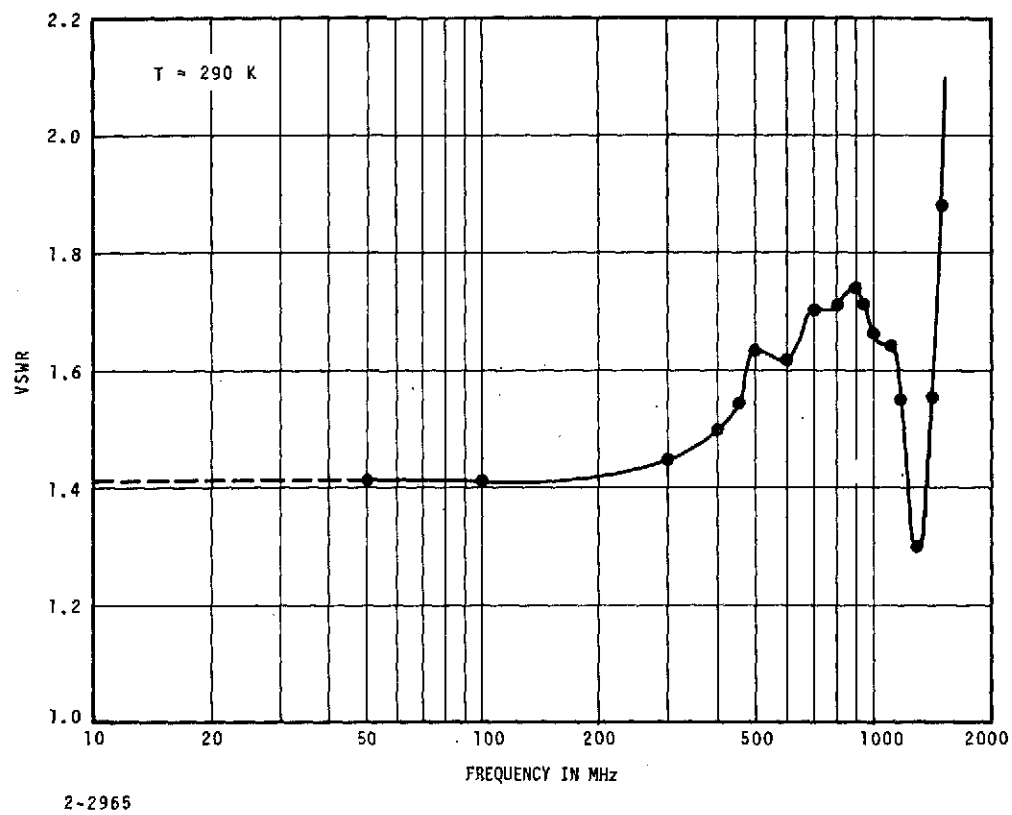


Figure 8. Measured Frequency Response of a Photomixer Housing

TABLE II. CALCULATED AFFECT OF SHUNT CONDUCTANCE VARIATIONS ON PHOTOMIXER
3-dB FREQUENCY RESPONSE

Applied Voltage V_B (mV)	Normalized Conductance* $G_D^{-1} \quad G_{D(400)}^{-1}$	Square Root of Normalized Conductance (proportional to f_c)	Deviation of Measured Cutoff Frequency* from $f_c = K (V_B)^N$ Relationship
-200	1.5	1.22	1.04
-300	1.14	1.06	1.05
-400	1.0	1.0	1.0
-800	0.642	0.80	0.742
-1000	0.535	0.728	0.742

* The photomixer conductances and 3-dB cutoff frequencies are normalized to the measured values of 1400 ohms and 560 MHz for $V_B = -400$ mV.

Based on these considerations, it appears that the change of photomixer shunt conductance with bias voltage may be the principal cause of the frequency deviation from the expected $f_c = K (V_B)^N$ relationship whereas the affect of photomixer housing resonance will have an insignificant affect at IF's below 1 GHz.

The measured 3-dB cutoff frequency which is approximately 850 MHz at $V_B = -800$ mV is in excellent agreement with reported data (reference 6 and 7) on previously developed PV-HgCdTe photomixers.

E. PHOTOMIXER HOUSING

A housing/coaxial adapter previously designed and developed jointly by AIL and the photomixer manufacturer on a previous NASA sponsored program was used to house the wideband photomixer. Figure 9 shows the photomixer housing/coaxial adapter.

The photomixer housing is hermetically sealed, provides efficient infrared transmission at $10.6 \mu\text{m}$, provides RFI immunity, and has been environmentally tested under a previous NASA program (reference 4). The natural cutoff frequency of the photomixer housing used on this program is estimated to be greater than 1500 MHz based on the photomixer frequency response measurement data.

F. IF PREAMPLIFIER

The wideband IF preamplifier used in the heterodyne receiver has been designed to provide low noise performance over the entire 5 to 1700 MHz frequency range. The measured IF preamplifier characteristics are as follows:

- Gain 40 dB
- Bandwidth 5 to 1700 MHz
- Noise Factor ≈ 4 dB
(reference 8)
- 1-dB Gain Compression +6 dBm

The dc bias for the wideband photomixer is introduced through a coaxial cable which is used to couple the IF beat frequency from the photomixer to the preamplifier. The input impedance and noise factor of the IF preamplifier have been optimized near 1200 MHz.

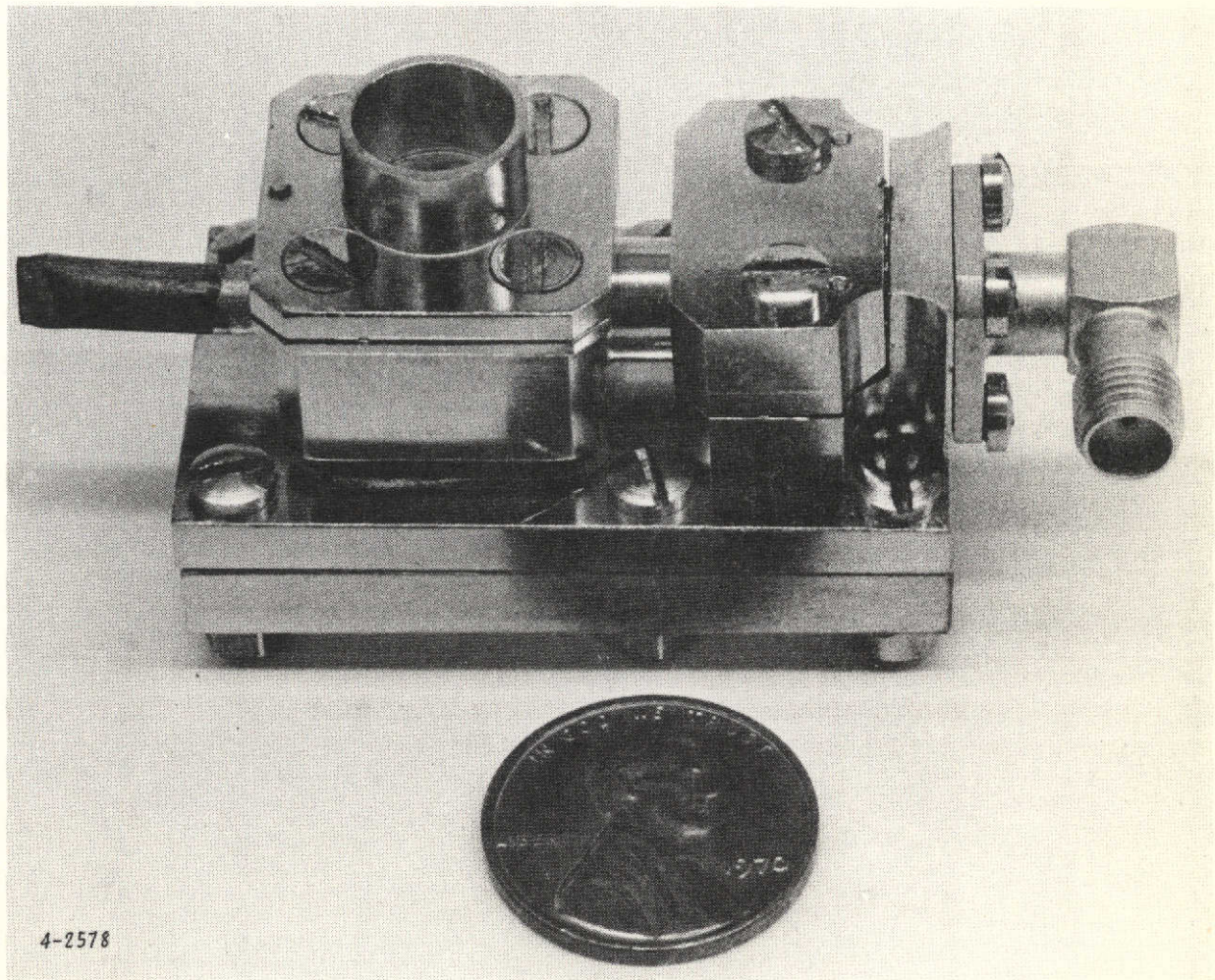


Figure 9. Space Quality Photomixer Housing

III. HETERODYNE RECEIVER PERFORMANCE

A. RECEIVER SENSITIVITY

The wideband infrared heterodyne receiver has been evaluated in a unique laboratory setup which employs two CO₂ lasers operating on their P-20 transitions at 10.59 μm . The photomixer was tested at operating temperatures between 77 and 140 K, and the receiver sensitivity has been measured as a function of laser LO power and dc bias power.

The heterodyne measurement setup employs two single-frequency cervit-cavity CO₂ lasers that serve as signal and LO sources, respectively. They deliver about 1 W CW each, operate on the same vibrational rotational line, and are locked in frequency at the desired IF offset, for example, 30 MHz, by sampling the laser outputs by two beamsplitters and mixing them in a separate p-type PC-HgCdTe detector. A 30-MHz discriminator generates an error signal, which is fed to the piezoelectric tuning stack of one of the lasers. Other IF's up to 40 MHz can be conveniently generated by adding an RF mixer and injecting an appropriate RF signal into the AFC loop. The main LO and signal beams illuminate the mixer element and are shaped individually by means of appropriate irises and lenses to obtain the desired diffraction-limited illumination.

A key consideration in receiver evaluation is the measurement of absolute infrared signal power. This is achieved by a substitution method whereby a high-reflectance mirror is inserted in the signal path to deflect the signal radiation to a room-temperature bolometer having a broad spectral response. The bolometer responsivity is calibrated using both a 500 K black-body source and a thermopile. To ensure accuracy, the bolometer is located in the same focal plane as the mixer. To eliminate errors due to nonuniform illumination, the bolometer is physically smaller than the mixer and a relatively broad signal beam is employed.

The noise equivalent power (NEP) for a reverse-biased photovoltaic infrared heterodyne receiver, defined as the signal power required to achieve a unity IF signal-to-noise ratio, is given (reference 2) by:

$$\text{NEP} = \frac{h\nu B}{\eta} \left\{ 1 + \frac{2k (T_m + T'_{IF}) G_D}{q I_0} \left[(1 + R_S G_D) + \frac{\omega^2 R_S C_D^2}{G_D} \right] \right\} \quad (6)$$

and is reducible to

$$\text{NEP} = \frac{h\nu B}{\eta} + \frac{k (T_m + T'_{\text{IF}}) B}{G} \quad (7)$$

where

η = photomixer quantum efficiency

k = Boltzmann's constant

T_m = physical temperature of the photomixer

T'_{IF} = effective input noise temperature of the IF preamplifier
 $= f (G_D^{-1})$

The available conversion gain of a reverse biased PV photomixer is given (reference 2) by:

$$G = \frac{(\eta q / h\nu)^2 P_{\text{LO}}}{2 G_D \{1 + (f/f_c)^2\}} \quad (8)$$

where

f = IF angular frequency

The first term in equation 7 represents the quantum noise contribution of the heterodyne receiver and can be expressed as the minimum detectable power $P_{\text{MIN}} = h\nu B / \eta$. The second term in equation 7 is related to the photomixer gain and the thermal noise in the photomixer and IF preamplifier.

Heterodyne receiver sensitivity measurements of the PV-HgCdTe photomixer/IF preamplifier front end have been carried out at a variety of photomixer dc bias voltages for a photomixer temperature of 77 K and an IF offset of 20 MHz. Figure 10 shows the measured heterodyne receiver NEP data for $V_B = -400$ and -800 mV. The photon energy ($h\nu$) at $\lambda = 10.6 \mu\text{m}$ is 1.87×10^{-20} W/Hz as compared to the measured receiver NEP of approximately 10^{-19} W/Hz at an IF of 20 MHz which corresponds to a quantum noise factor (reference 5) of 7.3 dB. The quantum noise factor begins to degrade for $\text{IF} > 550$ MHz.

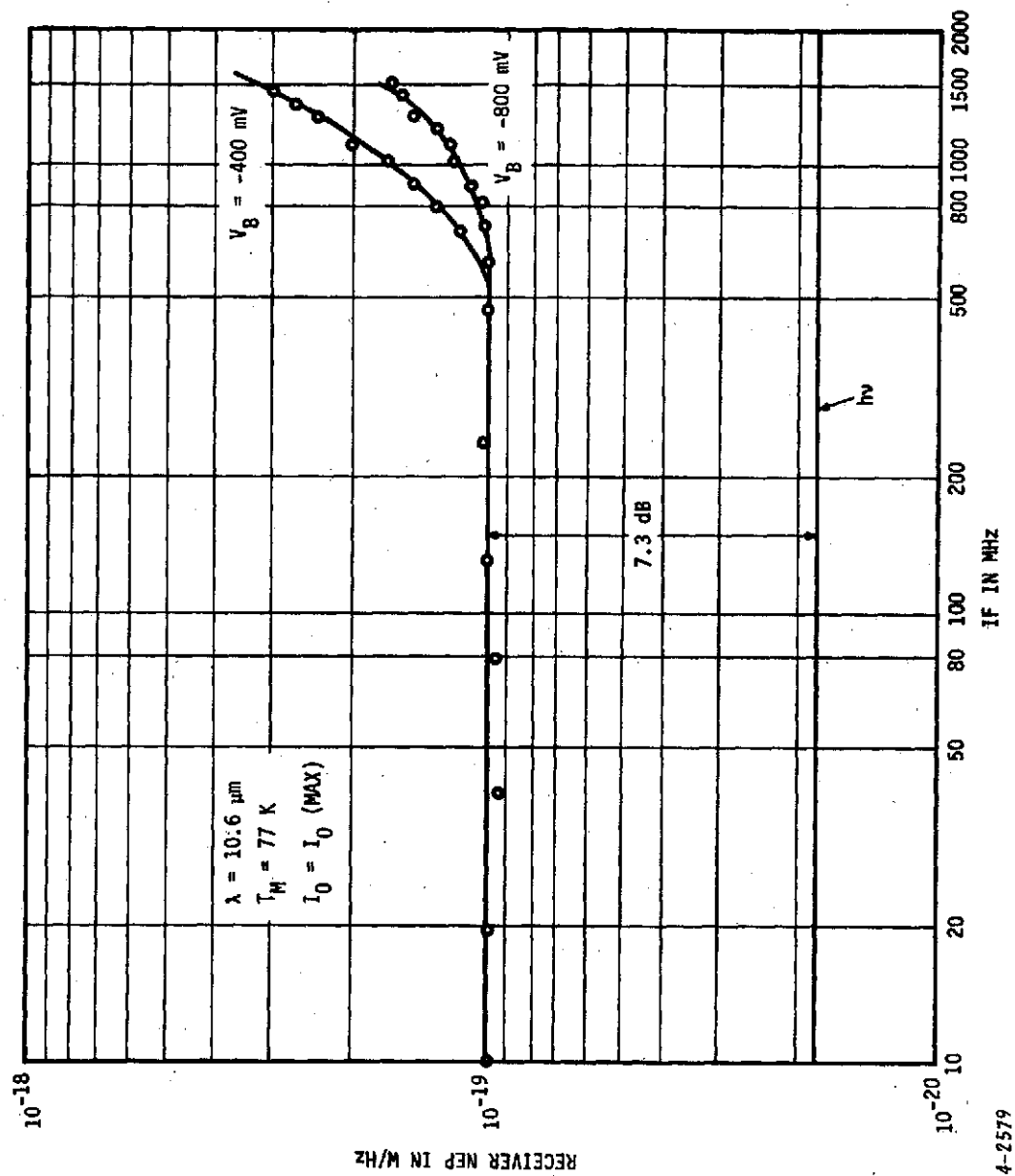


Figure 10. Measured Heterodyne Receiver Sensitivity for $V_B = -400$ and -800 mV

For an applied bias voltage of $V_B = -800$ mV, and $I_O \approx 1$ mA, the photomixer 3-dB cutoff frequency is approximately 850 MHz (Section II, Table I) and therefore the receiver sensitivity exhibits a slight degradation in receiver sensitivity above 800 MHz due to a rolloff in the photomixer gain (equation 8). For $V_B = -400$ mV and $I_O \approx 1.34$ mA, the photomixer 3-dB cutoff frequency is about 560 MHz and therefore the receiver NEP begins to show some degradation above 500 MHz. For wideband heterodyne receiver operation at IF's up to 1500 MHz, a bias voltage $V_B = -800$ mV appears to be a suitable voltage level. In order to minimize the degradation due to thermal noise contributions in the receiver, the IF preamplifier was optimized at an IF near 1200 MHz. The receiver NEP at 1500 MHz is 1.65×10^{-19} W/Hz for $V_B = -800$ mV and 3.2×10^{-19} W/Hz for $V_B = -400$ mV.

The techniques employed for receiver sensitivity evaluation over the IF range of 10 to 40 MHz was through direct measurements, by fixing the frequency offset of the two plane wave CO_2 lasers in the heterodyne test setup. The receiver sensitivity for $\text{IF} > 40$ MHz is measured by establishing the shot and thermal noise contributions in the heterodyne receiver and normalizing these results to the direct NEP measurements at $\text{IF} = 20$ MHz. This technique has been previously verified by independent measurements with a tunable diode laser source.

The photomixer shunt conductance varies with dc bias voltage (Figure 3) and therefore there is a corresponding variation of photomixer dark current with bias voltage. Since the maximum permitted current in the photodiode is fixed, the maximum permitted laser LO induced photocurrent will also vary with applied dc bias voltage. Table III gives the measured receiver NEP as a function of applied dc bias voltage for the case of maximum LO induced photocurrent. The IF preamplifier was optimized for operation at $V_B = -800$ mV and $\text{IF} = 1200$ MHz.

The measured receiver sensitivity over the reverse bias voltage range from -200 to -800 mV varied between 1.0 and 1.2×10^{-19} W/Hz at $T_m = 77$ K and for a 20-MHz IF offset. As can be seen from Table III, the photomixer reverse shunt resistance and the maximum LO induced photocurrent both decreased with increasing photomixer bias voltage. These variations in shunt resistance and LO induced photocurrent appear to have a compensating effect since (a) the decreasing shunt resistance improved the impedance match between the photomixer and IF preamplifier and reduces the effective input noise temperature (T'_{IF}) of the IF preamplifier, and (b) the decreasing photo-induced current and reverse shunt resistance both reduce the photomixer conversion gain (equation 6).

TABLE III. MEASURED INFRARED HETERODYNE RECEIVER SENSITIVITY FOR A PV HgCdTe PHOTOMIXER TEMPERATURE OF 77 K AND A 20-MHz IF OFFSET.

V_B (mV)	G_D^{-1} (ohms)	I_o^* (mA)	NEP $\times 10^{-19}$ W/Hz
-200	2100	1.44	~ 1.2
-400	1400	1.34	~ 1.1
-600	1125	1.2	~ 1.1
-800**	900	1.0	~ 1.0
-1000	750	0.74	~ 1.1

* These are the maximum permitted laser LO induced photocurrents and are fixed by the photomixer manufacturers specifications.

** The IF preamplifier has been optimized for operation with the photomixer biased to $V_B = -800$ mV.

Measurements of the variation of heterodyne receiver sensitivity with LO induced photocurrent have been carried out for several levels of applied bias voltage. The measured results indicate that for the maximum value of photoinduced current used, the receiver NEP continued to improve with increasing LO power and therefore it appears that the ultimate condition of $NEP \approx P_{min}$ has not been achieved. Since the maximum photocurrent in the photomixer is fixed by the manufacturers specifications, further improvements in receiver sensitivity can only be realized by reducing the thermal noise contribution of the IF preamplifier.

B. LASER LOCAL OSCILLATOR POWER

For a reverse biased photovoltaic photomixer operating in the flat portion of its frequency response ($f < f_c$), quantum-noise-limited heterodyne receiver operation is obtained when

$$I_o \gg \frac{2k (T_m + T_{IF}') G_D}{q} \quad (9)$$

or

$$P_{LO} \gg \frac{2k (T_m + T_{IF}') G_D h\nu}{q^2 \eta} \quad (10)$$

When the terms on the left side and the right side of inequalities 9 or 10 are equal, the thermal noise of the heterodyne receiver degrades the system sensitivity by exactly 3 dB.

Measurements on the variation of receiver NEP with photoinduced current I_o were carried out using the wideband PV-HgCdTe photomixer. Figure 11 shows results for $IF = 20$ MHz, $T_m = 77$ K, $V_B = -600$ mV, and $I_D = 0.3$ mA. The data indicates that the receiver sensitivity is approaching its quantum-noise-limited value of $\frac{h\nu B}{\eta}$ for a maximum photoinduced current of $I_{o(max)} = 1.20$ mA which corresponds to an LO power density of approximately 836 mW/cm^2 .

The minimum receiver sensitivity measured at $IF = 20$ MHz is

$$P'_{MIN} = \frac{h\nu B}{\eta'} = 10^{-19} \text{ W/Hz} \quad (11)$$

and corresponds to an effective quantum efficiency η' of about 19 percent. Additional applied laser LO power is expected to result in only slightly improved performance. Hence the quantum-noise factor (QF) as defined in reference 5 is:

$$QF = \frac{NEP}{h\nu B} = 7.3 \text{ dB} \quad (12)$$

The quantum-noise factor can be considered as a figure-of-merit which describes quantitatively how closely a given receiver approaches the theoretical sensitivity level.

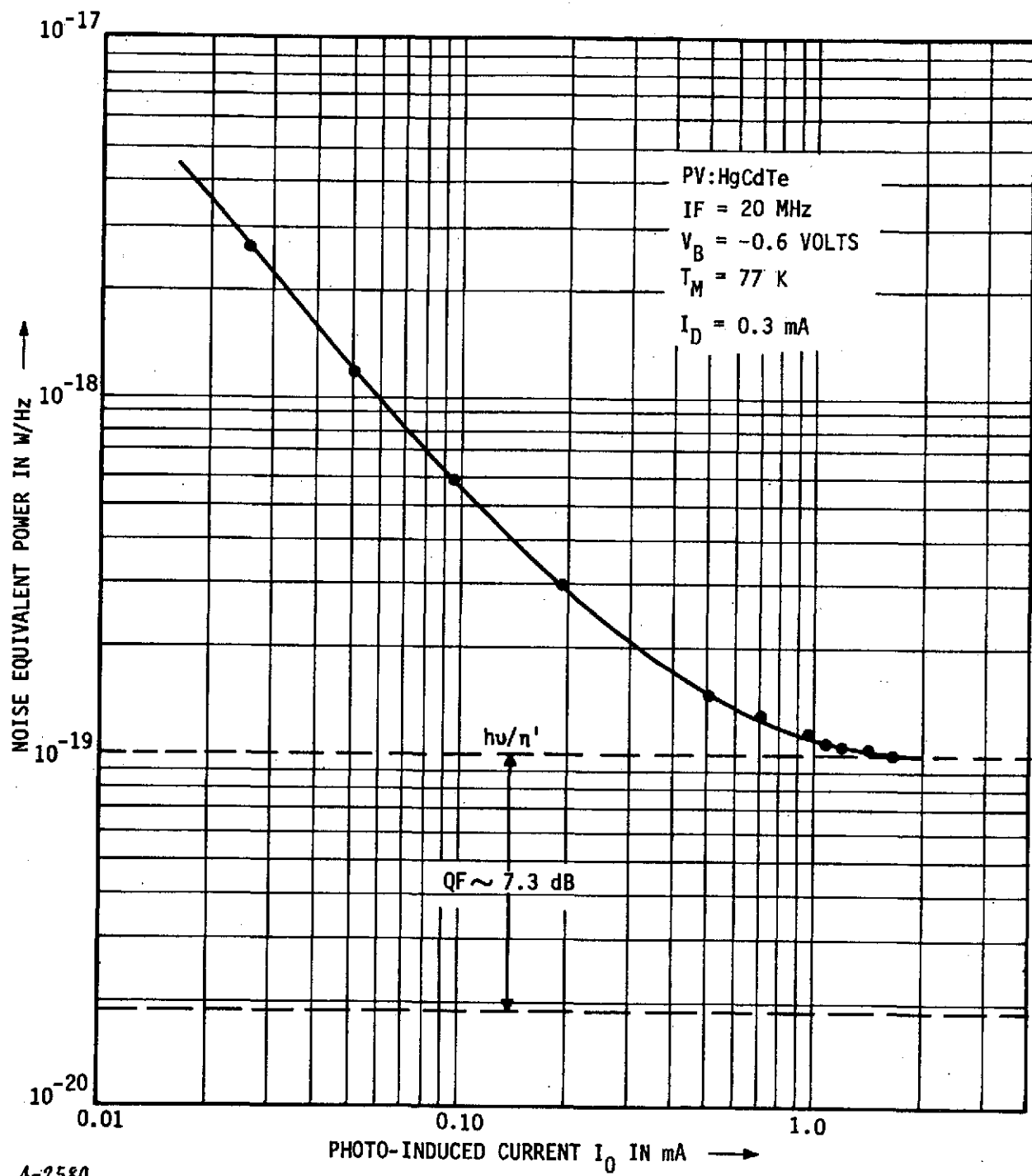


Figure 11. Measured Heterodyne Receiver Sensitivity of PV HgCdTe Photomixer/IF Preamplifier as a Function of Photoinduced Current

C. DC BIAS POWER

The optimum level for reverse dc bias voltage for the wideband photomixer is selected to:

- Provide a sufficiently large photomixer frequency response (Figure 7 and Table I)
- Provide a low forward-to-reverse resistance ratio ($R_S G_D \ll 1$)
- Reduce the photomixer output impedance to ease matching to a wideband IF preamplifier
- Minimize sensitivity degradation at the lower IF's due to contact ($1/f$) noise contributions (Section II-B)
- Permit efficient heterodyne operation over an extended range of photomixer temperatures
- Minimize photomixer dark current contribution

An applied bias voltage of -800 mV appeared to be an optimum value for the wideband photomixer, and hence, was used in this 10.6 μ m infrared heterodyne receiver.

IV. HETERODYNE RECEIVER PERFORMANCE AT ELEVATED PHOTOMIXER TEMPERATURE

For spacecraft applications, the infrared photomixer will be mounted in a radiative cooler. Since the operating temperature of the radiative cooler may vary between 90 and 120 K, the receiver performance has been evaluated over a wide range of photomixer temperatures.

A. PHOTOMIXER CHARACTERISTICS

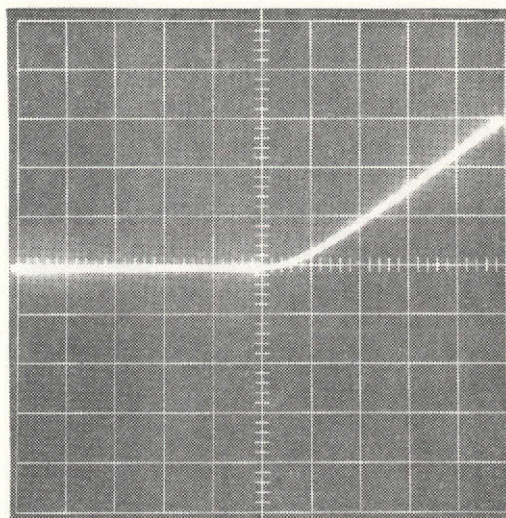
The position of the spectral peak for PV HgCdTe photomixers shifts toward shorter wavelengths as the temperature of the photomixer is increased (reference 5). Since the spectral response of the wideband photomixer peaks near $10.85 \mu\text{m}$ for $T_m = 77 \text{ K}$, the photomixer quantum efficiency at $10.6 \mu\text{m}$ is expected to degrade for $T_m > 100 \text{ K}$ due to this shift in the photomixer response.

The current-voltage characteristics of the wideband photomixer were measured for photomixer temperatures between $T_m = 77 \text{ K}$ and 130 K . Figure 12 shows the measured I-V characteristics for $T_m = 77 \text{ K}$ and 130 K and indicates a horizontal shift of the "knee" portion of the photomixer response curve near zero bias and an increase in the saturation current as the photomixer temperature is increased above 77 K .

Further detailed measurements of the I-V response characteristics in the photomixer were carried out to obtain the slope resistance over the 77 K to 130 K temperature range (Figure 13). With low negative bias ($V_B \leq -400 \text{ mV}$) the slope resistance increases to a maximum value at photomixer temperatures of 110 K and above, while for larger reverse bias voltages ($V_B \geq 0.4 \text{ V}$), the slope resistance appears to remain nearly constant over the measured temperature range. Therefore it appears to be desirable to operate the mixer at bias voltages greater than $V_B = -400 \text{ mV}$ so as to avoid operation near the "knee" portion of the I-V curve. This will furthermore minimize the input impedance requirements on the IF preamplifier while allowing operation over an extended temperature range. It should be pointed out however, that such factors as quantum efficiency, cutoff, frequency, induced shot noise, and sensitivity must also be considered in conjunction with the operating temperature parameter.

$T_M = 77 \text{ K}$

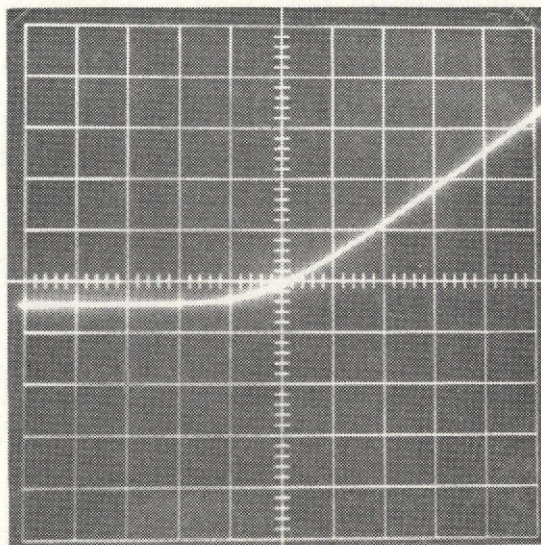
2 mA/DIV



0.1 V/DIV

$T_M = 130 \text{ K}$

2 mA/DIV



0.1 V/DIV

4-2640

Figure 12. Measured Current Voltage Characteristics of a Wideband PV HgCdTe Photomixer at 77 K and 130 K

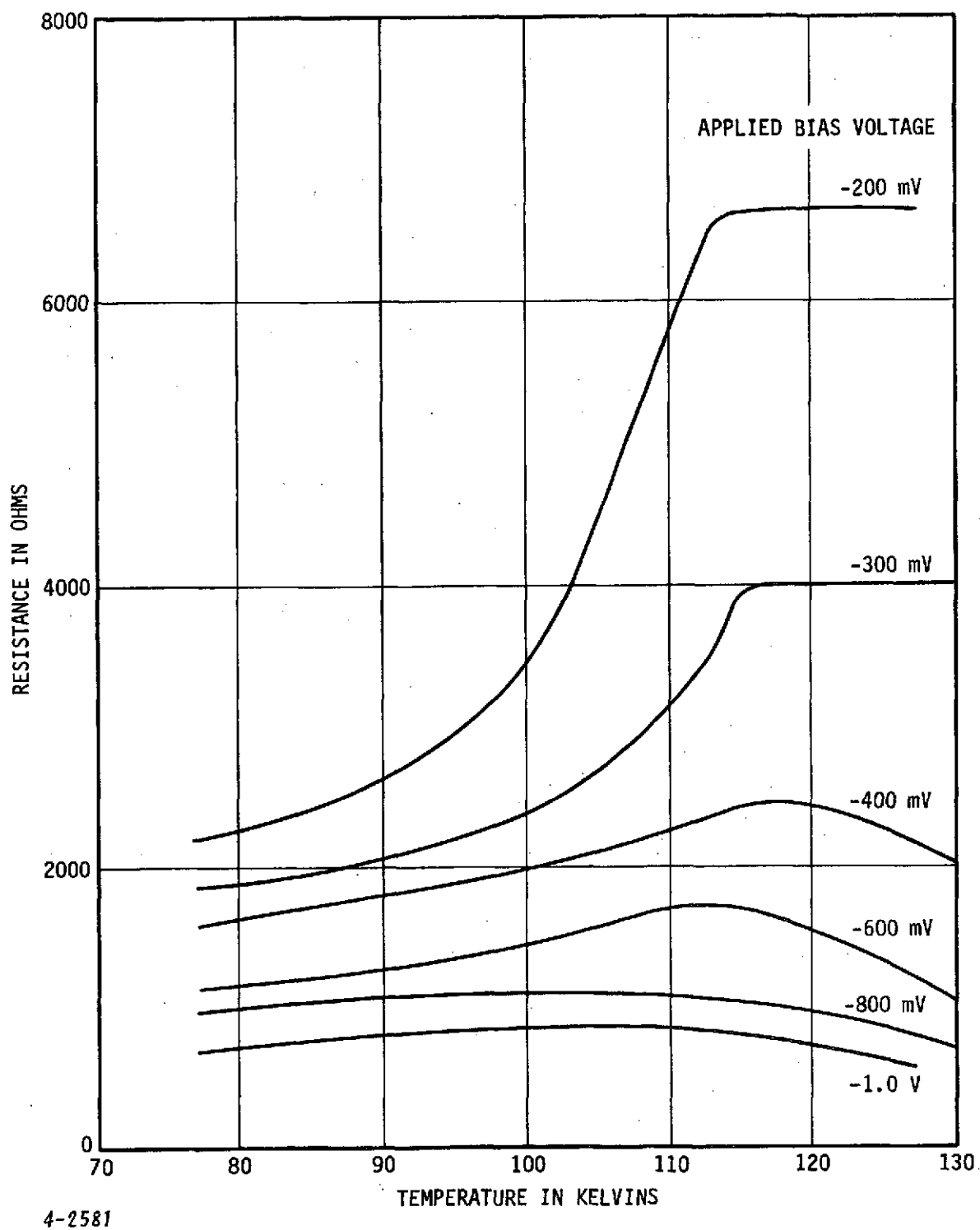


Figure 13. Photomixer Slope Resistance Versus Temperature with Reverse Bias Voltage as a Parameter

B. LASER LO INDUCED PHOTOCURRENT

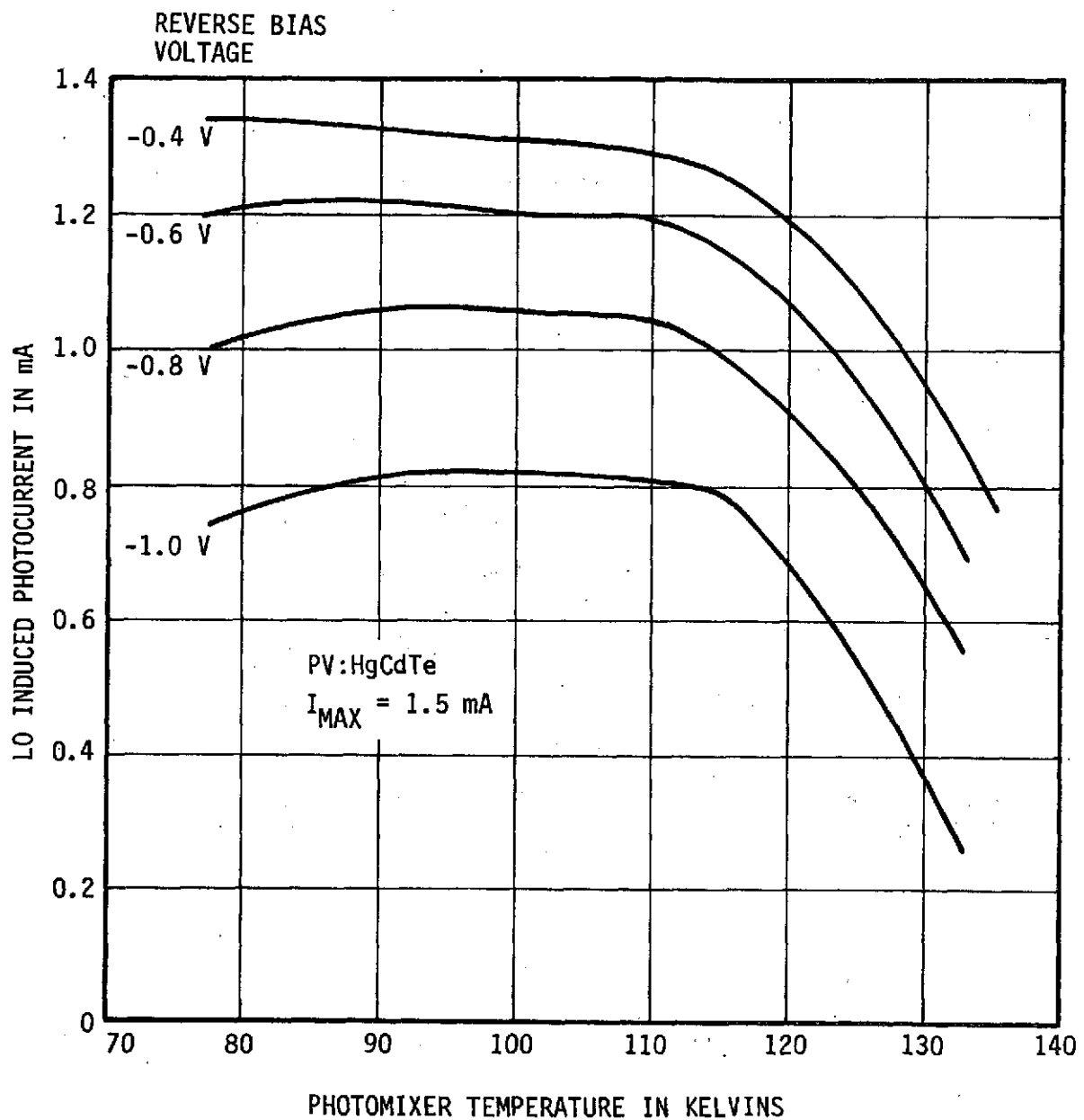
Measurements were carried out on the wideband photomixer to determine the maximum allowable laser LO induced photocurrent I_o at various bias voltages over the 77 to 130 K temperature range. Based on the photomixer specifications, the maximum current (made up of the sum of the dark and laser LO induced photocurrent) is approximately 1.5 mA. The measured results (Figure 14) exhibit a rapid decrease in allowable photocurrent at photomixer temperatures above 110 K. As expected for a constant operating photomixer temperature, an increase in bias voltage results in an increase of photomixer dark current and in a corresponding decrease of the allowable LO induced photocurrent. The heterodyne receiver sensitivity is a function of photomixer conversion gain which in turn is proportional to the LO induced photocurrent. Hence, to assure optimum performance, careful analysis and experimentation must be carried out on the interrelationship between the bias voltage, the LO induced photocurrent, the cutoff frequency, and the photomixer sensitivity, as described previously in this report.

Based on the results it appears that an applied bias voltage of $V_B = -800$ mV is within the optimum operating region for the wideband heterodyne receiver. The resultant maximum I_o is 1 mA at 77 K, increases to 1.05 mA near 100 K and drops to 0.9 mA at 120 K. The 3-dB cutoff of the photomixer at $V_B = -800$ mV is approximately $f_c = 850$ MHz for T_m between 77 and 130 K (Table I).

C. PHOTOMIXER CUTOFF FREQUENCY

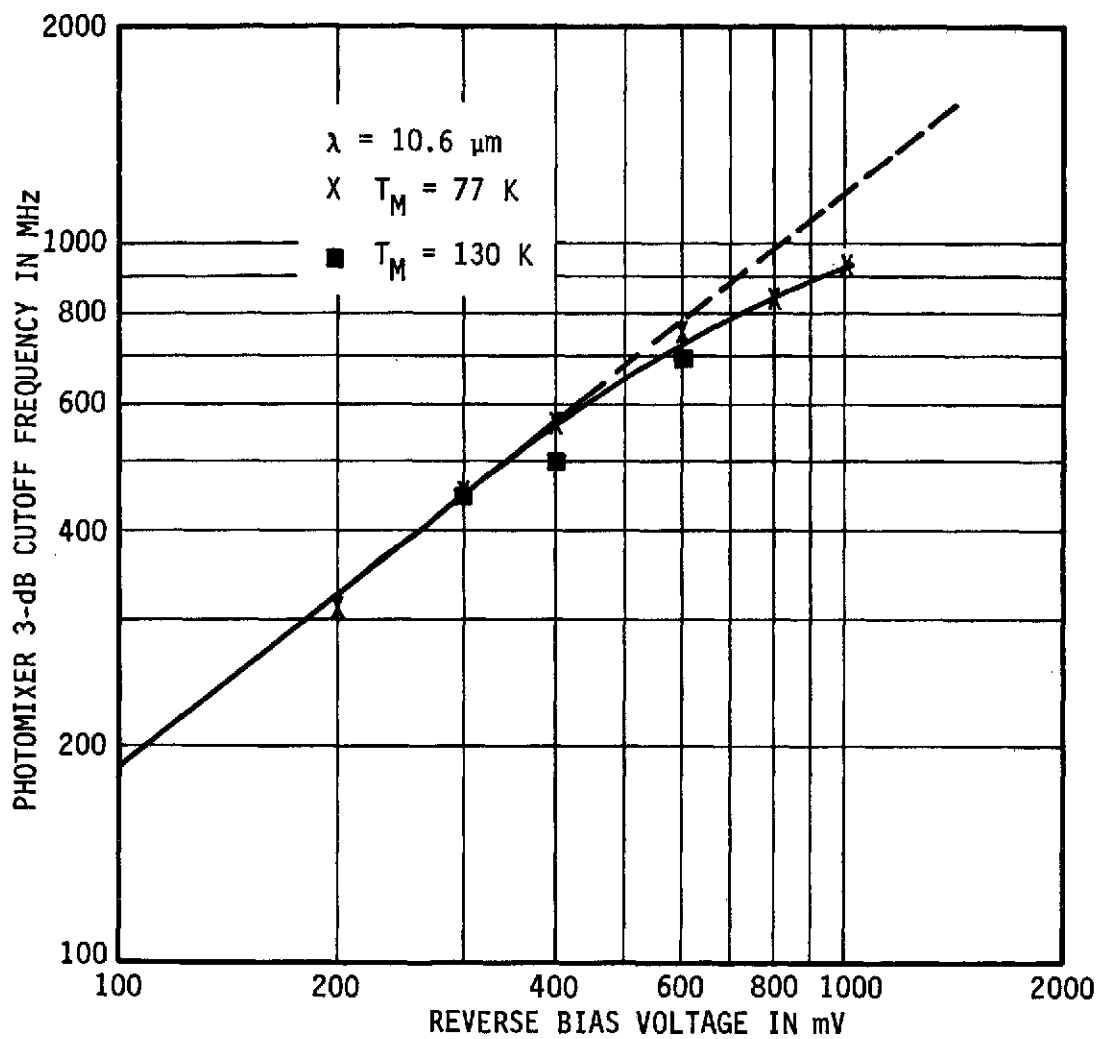
Measurements of the frequency response of the wideband PV HgCdTe photomixer were carried out for a variety of bias voltages V_B and photomixer temperatures T_m . Figure 15 shows the variation of the measured 3-dB cutoff frequency with bias voltage at $T_m = 77$ K and 130 K. The measured cutoff frequency was 310 MHz at $V_B = -200$ mV and increased to 970 MHz at $V_B = -1.0$ volt.

The measured data (Table IV) demonstrates that the cutoff frequency variation with reverse bias is essentially independent of mixer temperature over the 77 K to 130 K temperature range. This result is in agreement with previous measurements (reference 2) on PV HgCdTe photomixers.



4-2582

Figure 14. Maximum Laser LO Induced Photocurrent as a Function of Photomixer Temperature with Photomixer Bias Voltage as a Parameter



4-2583

Figure 15. Measured 3-dB Cutoff Frequency Versus Bias Voltage for Wideband PV HgCdTe Photomixer

TABLE IV. VARIATION OF PV HgCdTe PHOTOMIXER 3-dB CUTOFF FREQUENCY AS A FUNCTION OF BIAS VOLTAGE AND MIXER TEMPERATURE

Applied Bias Voltage (mV)	3-dB Cutoff Frequency (MHz)	
	$T_m = 77 \text{ K}$	$T_m = 130 \text{ K}$
-200	310	-
-300	460	450
-400	560	500
-600	750	720
-800	850	850
-1000	970	-

D. RECEIVER SENSITIVITY

The heterodyne receiver NEP was measured as a function of IF offset at photomixer temperatures of 109 K and 130 K with maximum incident laser LO power to simulate operation in a radiative cooler. The measured results (Figure 16) indicate that the NEP near 20 MHz for $V_B = -800 \text{ mV}$ is $1.5 \times 10^{-19} \text{ W/Hz}$ at $T_m = 109 \text{ K}$ and increases to $1.75 \times 10^{-19} \text{ W/Hz}$ at $T_m = 130 \text{ K}$. The receiver NEP improves slightly near IF = 700 MHz due to optimum impedance matching between the photomixer and the IF preamplifier, and then degrades slightly with increasing IF due to a decrease in the photomixer gain (equation 8). For an IF of 1500 MHz, the receiver NEP is $2.35 \times 10^{-19} \text{ W/Hz}$ at 109 K and increases to $3 \times 10^{-19} \text{ W/Hz}$ at 130 K.

Figure 17 shows measured data on the receiver NEP at IF = 20 MHz as a function of applied bias voltage with photomixer temperature as a parameter. Tables V and VI also present the measured data on receiver NEP's at IF = 20 MHz for $V_B = -400 \text{ mV}$ and -800 mV . As can be observed, the receiver NEP for IF = 20 MHz degrades rapidly for photomixer temperatures above $T_m = 134 \text{ K}$ for the particular PV HgCdTe photomixer under test. This is apparently due to the large dark currents near zero bias (Figure 18) which prevent efficient heterodyne operation.

A 5-inch semi-rigid stainless steel, 34-mil diameter 50 ohm coaxial cable was inserted between the photomixer and the IF preamplifier to simulate operation in a radiative cooler. The measured NEP appeared to be unaffected by the insertion of the cable.

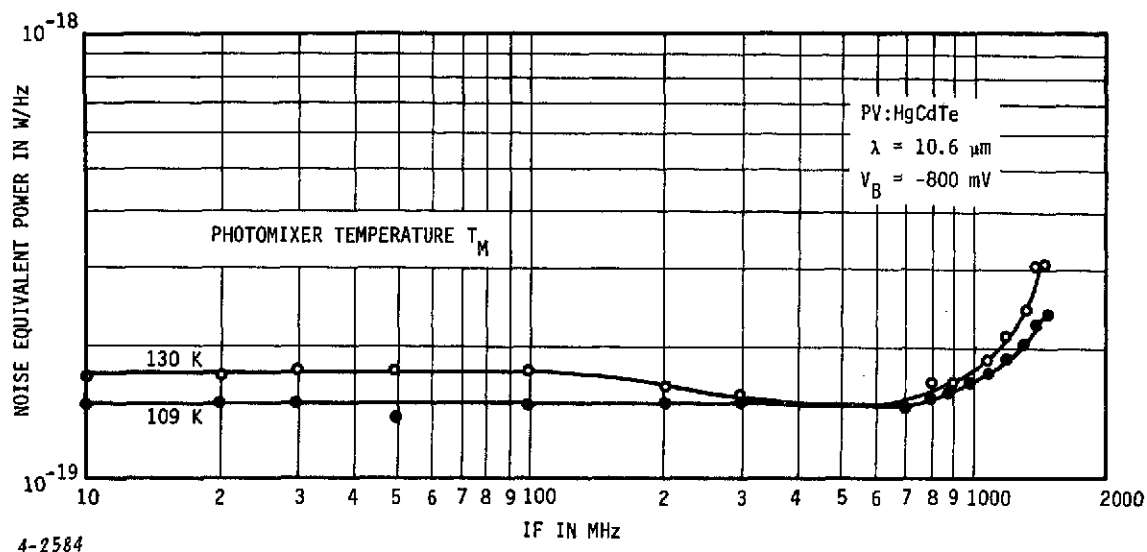


Figure 16. Heterodyne Receiver NEP Versus IF with Photomixer Temperature as a Parameter

TABLE V. MEASURED HETERODYNE RECEIVER SENSITIVITY AT PHOTOMIXER TEMPERATURES BETWEEN 77 K AND 137 K FOR IF = 20 MHz AND $V_B = -400 \text{ mV}$

Photomixer Temperature (K)	Heterodyne Receiver NEP $(\text{W/Hz}) \times 10^{-19}$
77	1.0
95	1.2
110	1.25
120	1.35
130	1.45
134	1.80
137	3.2

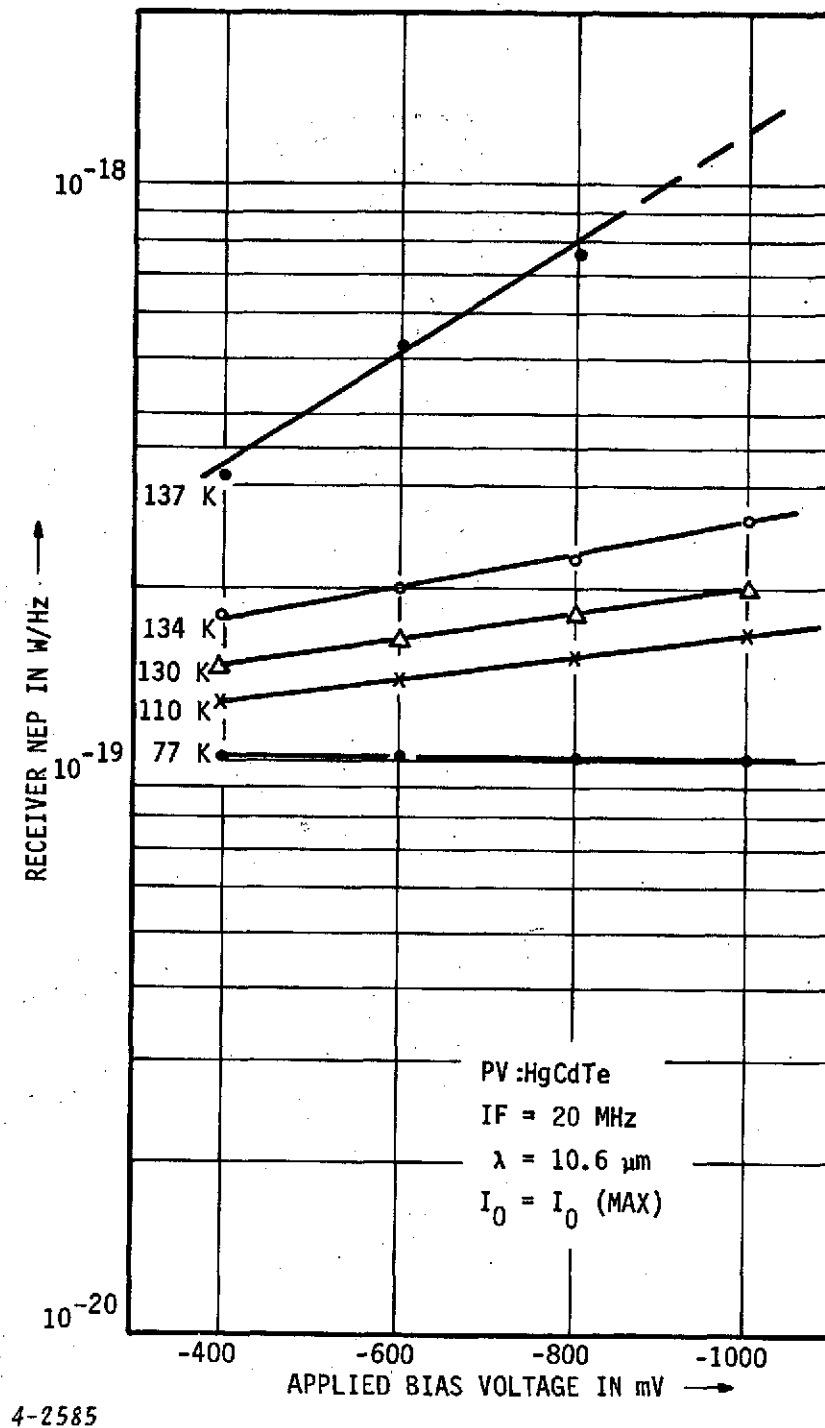
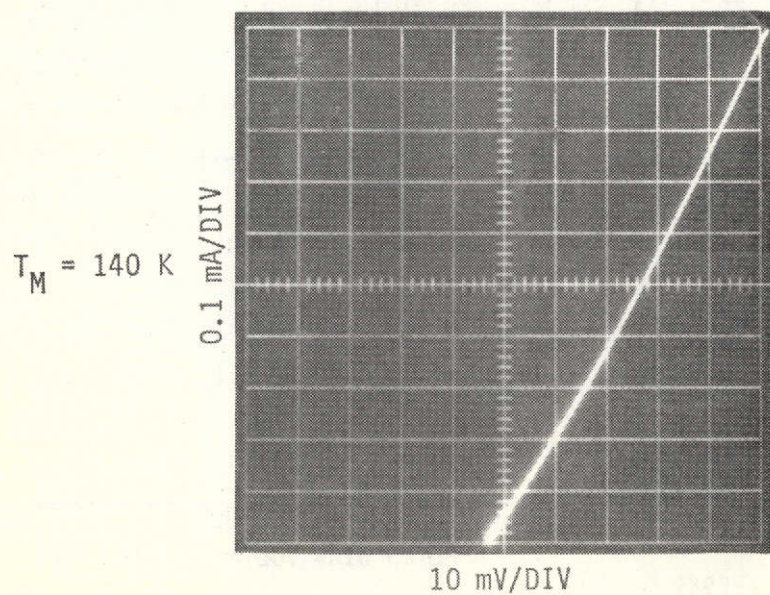
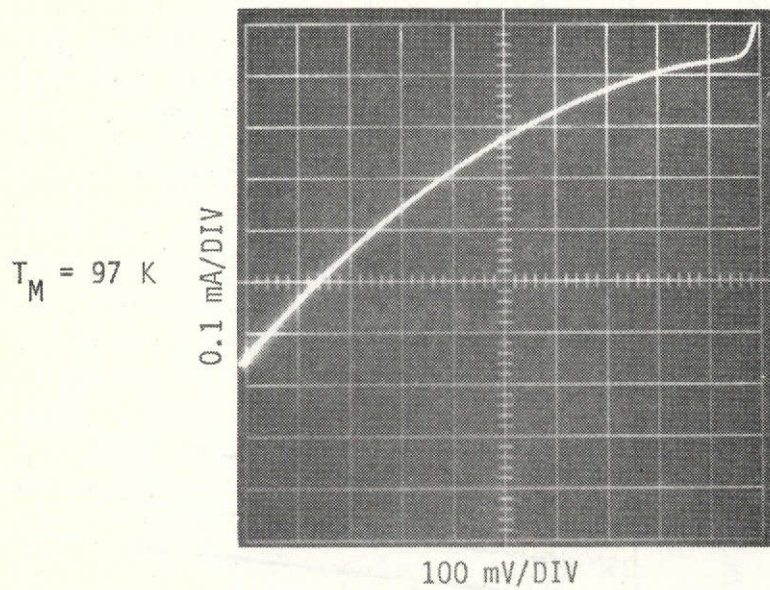


Figure 17. Measured Heterodyne Receiver Sensitivity as a Function of Applied Photomixer Bias Voltage with Photomixer Temperature as a Parameter



4-2586

Figure 18. Measured Reverse Current Characteristic of a Wide-band PV HgCdTe Photomixer at 97 K and 140 K

TABLE VI. MEASURED HETERODYNE RECEIVER SENSITIVITY
AT PHOTOMIXER TEMPERATURES BETWEEN 77 AND 147 K FOR
IF = 20 MHz AND $V_B = -800$ mV

Photomixer Temperature (K)	Heterodyne Receiver NEP (W/Hz) $\times 10^{-19}$
77	1.0
95	1.3
110	1.5
120	1.65
130	1.75
134	2.3
147	> 5

Based on these measurements, it appears that the maximum operating temperature of 134 K is limited by the dark current for this particular PV HgCdTe photodiode. However, work has recently been initiated toward achieving nearly quantum-noise-limited operation with PV HgCdTe photomixers cooled to temperatures of 146 K and above (references 9 and 10).

V. PACKAGED RECEIVER

The PV HgCdTe photomixer housing has been mounted in a variable temperature cooler and the wideband IF preamplifier and IF postamplifiers were mounted on the vacuum shroud of the cooler (Figures 19 and 20). Figure 21 shows a remote control panel which monitors photomixer current and bias voltage and provides photomixer overload protection as well as required power supplies.

A. VARIABLE TEMPERATURE COOLER

An open-cycle Joule-Thomson Cryo-Tip AC-1 Refrigerator manufactured by Air Products Corporation is used to cool the photomixer.

The basic components of the refrigerator include:

- a. Heat Exchanger -- The heat exchanger consists of finned tubing coiled about a mandrel to give efficient heat transfer. The photomixer is mounted on the copper tip of the heat exchanger and this surface is the only portion of the heat exchanger which reaches cryogenic temperatures.
- b. Cooler Control Panel -- The cooler control panel:
 - (1) Maintains a clean supply of nitrogen gas to the refrigerator
 - (2) Monitors the gas flow rate and controls the terminal temperature
 - (3) Protects the heat exchanger from excessive back pressures
 - (4) Evacuates the nitrogen supply lines conveniently during the startup period
- c. Vacuum Shroud -- To obtain cryogenic temperatures, the heat exchanger must operate in an evacuated volume obtained by use of the vacuum shroud. The shroud provides a vacuum-tight seal of at least 10^{-4} torr (0.1 μ m Hg) and a radiation shield is used to enclose the vacuum chamber and reduce heat losses.

- d. Flexlines and Regulator -- The flexlines, which contain the purified coolant (nitrogen gas), allow the photomixer to be oriented in any position while operating at cryogenic temperatures.

The manufacturer's specifications of the refrigerator are:

Heat exchanger type	Coiled finned tubing
Net refrigeration capacity	Up to 7 watts @ 77 K
Temperature range	68 to 200 K
Temperature control	0.1 K from 68 to 110 K
Cooldown time	5 to 30 minutes depending upon specimen mass, shielding, and flow rate

To obtain optimum refrigerator performance, such as minimum cool-down time and maximum refrigeration and minimum gas consumption, inherent system heat leaks must be minimized. To that end all cable lengths were kept to a minimum, indium shims were used to ensure good thermal paths, and a radiation shield composed of aluminized mylar was used to reduce radiation losses.

B. PHOTOMIXER-IF PREAMPLIFIER CONTROL PANEL

The photomixer-IF preamplifier control panel provides all the necessary instrumentation to energize and monitor the heterodyne receiver front end. Front panel switches are provided for energizing the system power, IF preamplifier power, and photomixer bias power. A digital voltmeter is available to monitor the photomixer bias voltage and current. A knob is also available to adjust the bias voltage.

A current overload circuit is employed to shut off the applied bias voltage when the current through the photomixer exceeds 1.5 mA. After a current overload condition, the bias voltage adjust is reduced to zero, by turning the mixer bias voltage adjust knob in the maximum counterclockwise direction. When the mixer bias reset button is depressed, the bias voltage can be reapplied.

C. OPERATING LEVELS

In normal operation, the photomixer is cooled to the desired temperature before the photomixer-IF preamplifier control panel is activated. The

bias voltage is then adjusted to be -800 mV and the dark current is recorded. * The laser LO power is then introduced, spatially centered, and adjusted to provide a total operating photomixer current of 1.5 mA (maximum), or less.

CAUTION

Laser LO power and dc bias power should never be applied to the photomixer until it has been cooled to cryogenic temperatures.

* The dark current is 0.5 mA for $V_B = -800$ mV and $T_m = 77$ K.

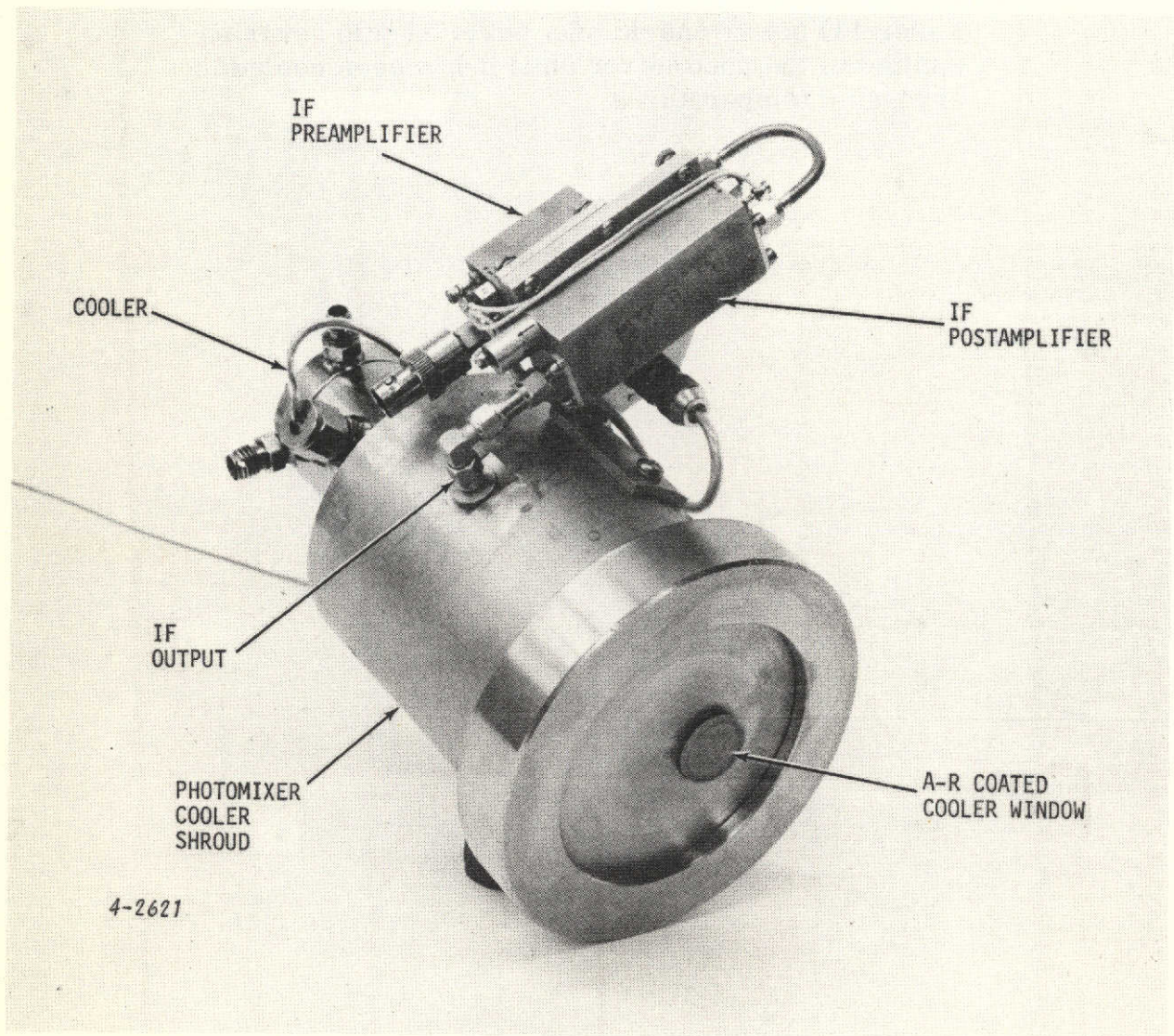


Figure 19. Photomixer Cooler with IF Preamplifier and IF Postamplifier

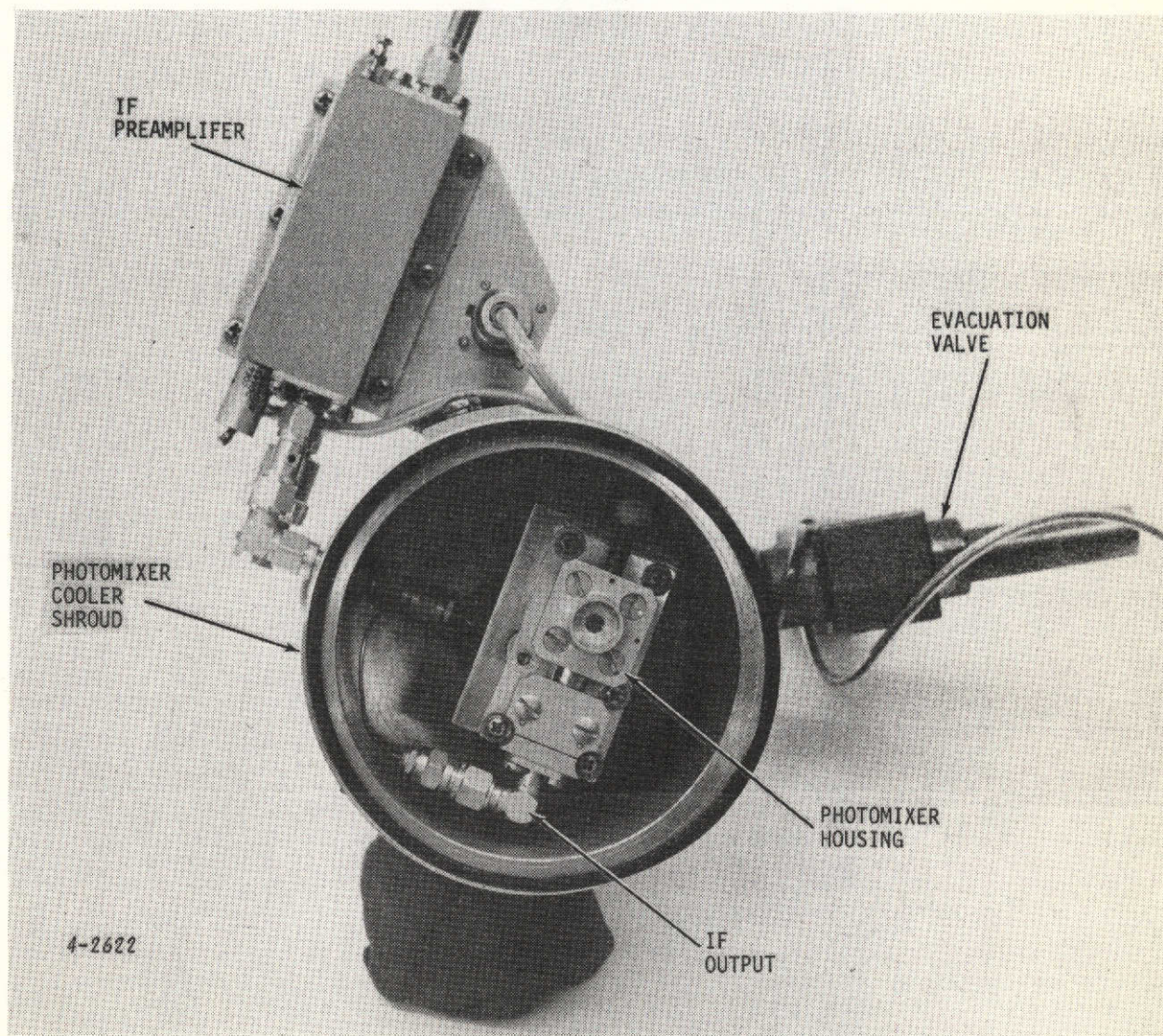


Figure 20. Photomixer Housing Mounted in Variable Temperature Cooler

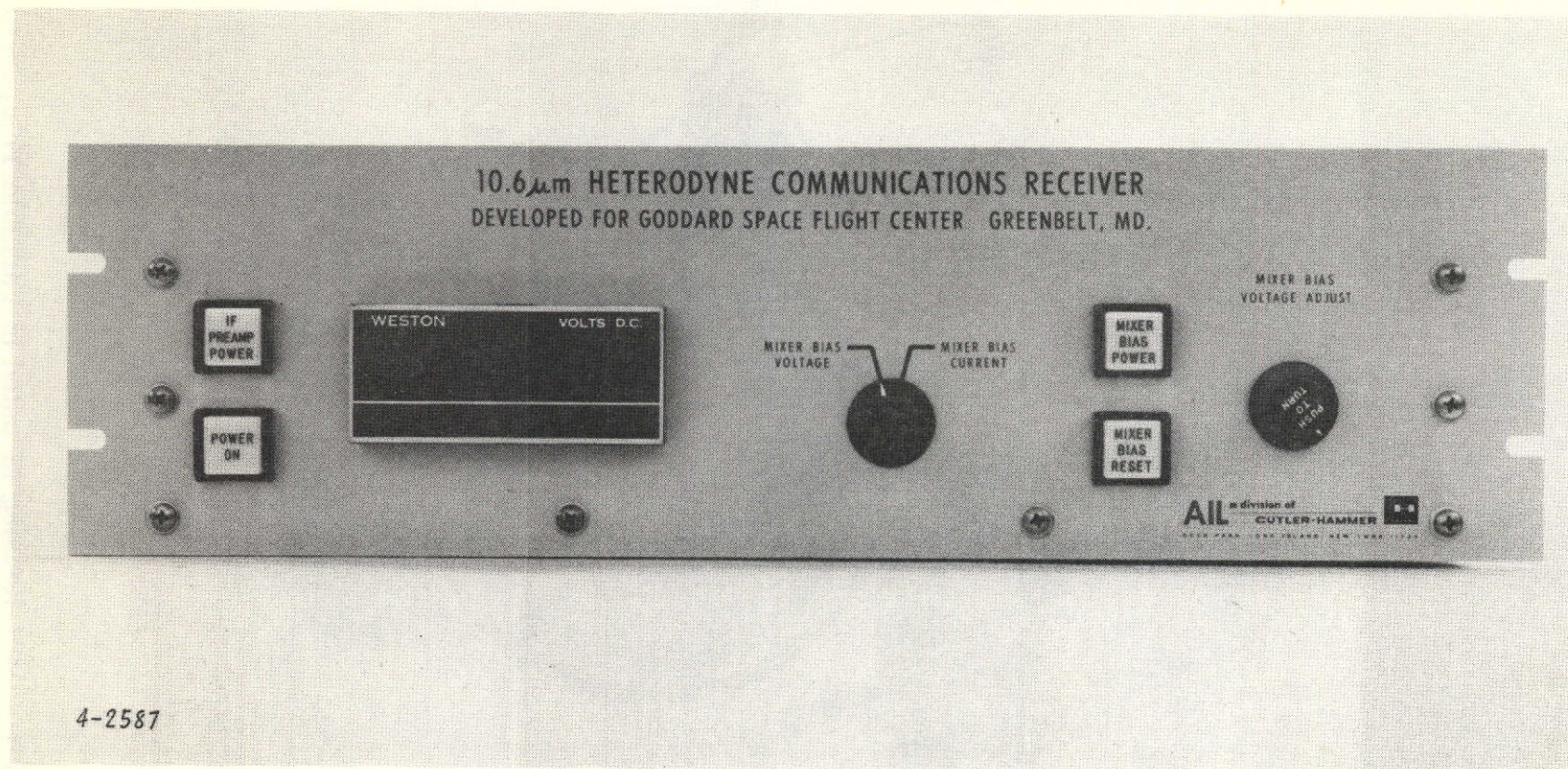


Figure 21. Remote Control Panel and Power Supplies

VI. CONCLUSIONS

Extensive analysis and measurements aimed at establishing the feasibility of developing a high-sensitivity, wide bandwidth 10.6- μm heterodyne receiver which operates over a wide range of photomixer temperatures has been completed. An infrared heterodyne receiver front end has been developed and tested for use in a space-to-ground CO₂ laser communications link.

The heterodyne receiver front end is made up of a variable temperature cooler which houses the photomixer housing, a wideband IF preamplifier, and a remote control panel. The measured receiver key characteristics include:

Optical wavelength	10.6 μm
IF response	5 to 1500 MHz
Photomixer operating temperature	77 to 130 K
Photomixer bias voltage	-800 mV
IF preamplifier gain	40 dB
Receiver sensitivity	NEP $\approx 10^{-19}$ W/Hz, IF = 20 MHz and $T_m = 77$ K $\approx 1.65 \times 10^{-19}$ W/Hz, IF = 1500 MHz, and $T_m = 77$ K $\approx 1.75 \times 10^{-19}$ W/Hz, IF = 20 MHz, and $T_m = 130$ K $\approx 3 \times 10^{-19}$ W/Hz, IF = 1500 MHz, and $T_m = 130$ K

Figures 22 and 23 show the complete CO₂ Laser Communications Receiver developed at AIL.

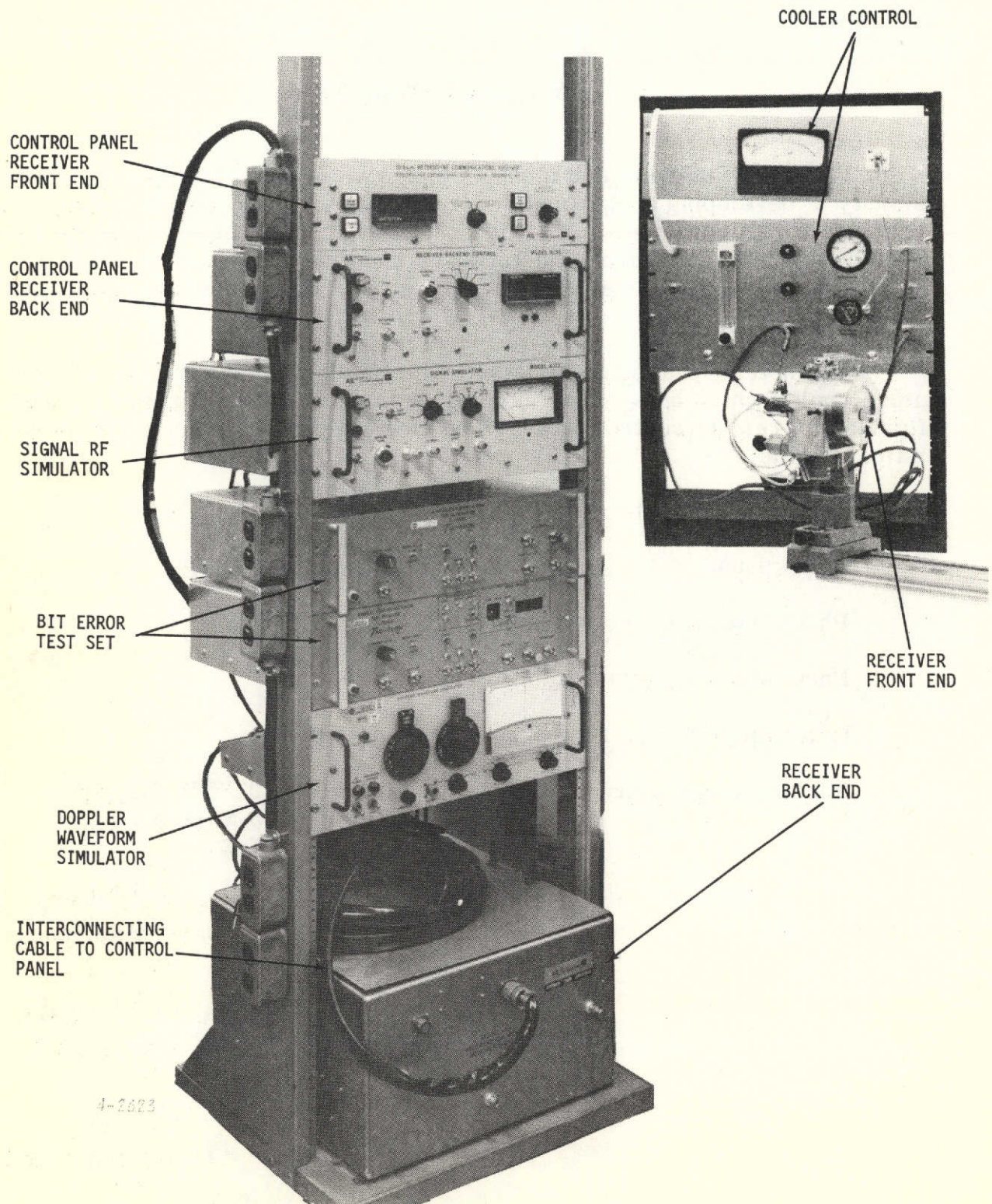


Figure 22. Complete CO₂ Laser Communications Receiver

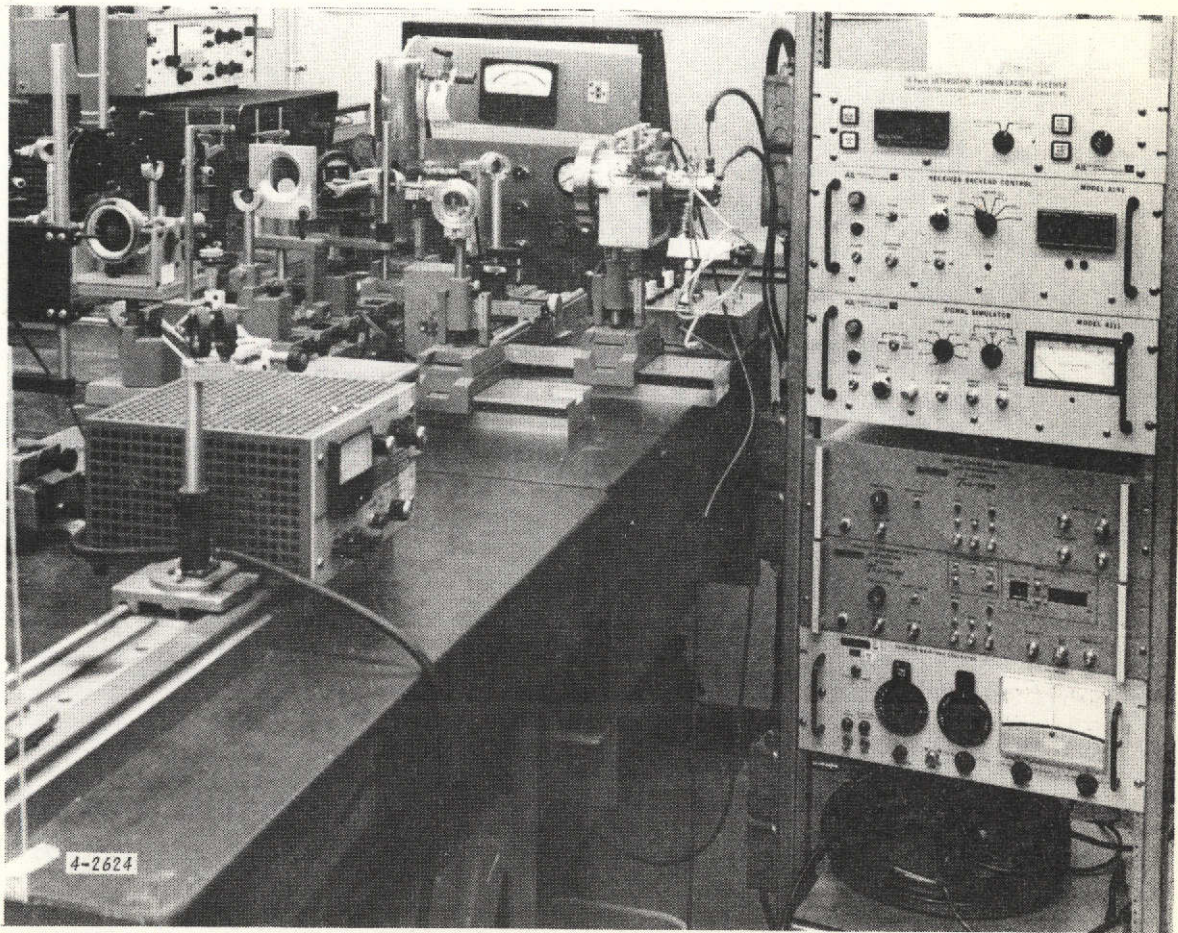


Figure 23. Complete CO₂ Laser Communications Receiver Mounted In Laboratory Test Setup

VII. REFERENCES

1. J. McElroy, N. McAvoy, H. Richard, T. McGunigal, and G. Schiffner, "Carbon Dioxide Laser Communications Systems for Near-Earth Applications," Proc IEEE Int Conf on Communications, p 22-27 to 22-37, San Francisco, 8-10 June 1970.
2. B. J. Peyton, A. J. DiNardo, G. K. Kanischak, F. R. Arams, R. A. Lange, and E. W. Sard, "High-Sensitivity Receiver for Infrared Laser Communications," IEEE Jour Quant Elect., QE-8, No. 2, p 252, February 1972.
3. T. Flattau and J. Mellars, "Wideband Infrared Receiver Backend," Final Report for NASA Contract NAS-5-23183, August 1974.
4. B. J. Peyton, "High Sensitivity Infrared 10.6- μ m Heterodyne Receiver Development," Final Design Report for NASA Contract NAS-5-11665, April 1972.
5. "Infrared Detectors," Vol 5 of "Semiconductors and Semi-metals," Chapters 5 and 10, Academic Press, 1970.
6. C. Verie and M. Sirieix, "Gigahertz Cutoff Frequency Capabilities of CdHgTe Photovoltaic Detectors at 10.6 μ m," IEEE Jour Quant Elect., QE-8, No. 2, p 180, February 1972.
7. D. L. Spears, T. C. Hartman, and I. Melngailis, "High Quantum Efficiency HgCdTe Photodiodes at 10.6 μ m," Proc IRIS Detector Specialty Group Meeting, April 1973, Washington, D. C.
8. IRE Subcommittee 7.9, "Description of Noise Performance of Amplifiers and Receiving Systems," Proc IRE, Vol S1, p 436-442, March 1963.
9. T. Koehler, "Mercury Cadmium Telluride 10.6-Micrometer Photodiode," Honeywell Radiation Center Interim Report on U.S. Army ECOM Program dated December 1973.
10. C. Burke and T. Koehler, "HgCdTe Photodiode Module for 10.6 μ m Heterodyne Detection at 170 K," to be published.